Fundamental understanding on the use of Bluetooth scanner as a complementary transport data

By

Ashish Bhaskar

Smart Transport Research Centre

School of Civil Engineering and Built Environment

Faculty of Built Environment and Engineering

Queensland University of Technology

Gardens Point Campus – S723

2 George St. GPO Box 2434, Brisbane QLD 4001, Australia

Phone: +61 7 3138 9985

e-mail: ashish.bhaskar@qut.edu.au

and

Edward Chung

Smart Transport Research Centre

School of Civil Engineering and Built Environment

Faculty of Built Environment and Engineering

Queensland University of Technology

Gardens Point Campus – P850

2 George St. GPO Box 2434, Brisbane QLD 4001, Australia

Phone: +61 7 3138 1143

e-mail: edward.chung@qut.edu.au

ABSTRACT

Literature is limited in its knowledge of the Bluetooth protocol based data acquisition process and in the accuracy and reliability of the analysis performed using the data. This paper extends the body of knowledge surrounding the use of data from the Bluetooth Media Access Control Scanner (BMS) as a complementary traffic data source. A multi-layer simulation model named Traffic and Communication Simulation (TCS) is developed. TCS is utilised to model the theoretical properties of the BMS data and analyse the accuracy and reliability of travel time estimation using the BMS data.

LIST OF KEYWORDS

- Bluetooth
- Traffic simulation
- Communication simulation
- Travel time
- Signalised network
- Bluetooth scanners
- Data

1 Introduction and Literature Review

Transport agencies collect data from multiple sources for various applications related to monitoring, management and control, planning and finance. Advancement of technology has resulted in the production of numerous data retrieval systems, ranging from traditional loop detectors to Vehicle Information and Communication Systems (VICS). These systems are broadly classified as: a) Fixed sensors (such as loops, Automatic Number Plate Recognition System (ANPR)) that provide traffic information at the location where the sensors are installed and b) Mobile sensors (such as GPS equipped vehicles, Automatic Vehicle Location (AVL)) that provide data for the entire journey of the vehicle equipped with such sensors.

In early 2000, researchers explored the use of Bluetooth (BT) technology for the automotive industry. Nusser and Plez (2000) presented the architecture of the Bluetooth network as an integral part of in-car communication and information systems. Researchers (Sawant et al., 2004, Murphy et al., 2002 , Pasolini and Verdone, 2002) have tested the proof-of-concept for the use of BT for Intelligent Transport System services, and have verified that the BT equipped devices in moving vehicles could be discovered.

Recently, there has been significant interest from transport agencies in exploiting the Bluetooth Media Access Control Scanner (BMS) as a complementary transport data source. The concept behind BMS is rather simple. A BMS scanner has a communication range (say

around 100 meters in radius) that we term as *zone*. The *zone* is scanned to read the Media Access Control addresses (MAC-ID) of the *discoverable* BT devices transiting within the *zone*. The MAC-ID is a unique, alpha-numeric string, that is communicated by the *discoverable* BT device. Most of the portable electronic devices such as mobile phones, car navigation systems, headphones, etc. are equipped with BT and its usage is increasing. Indeed, the strategic analytics of Special Interest Group (SIG)- an organisation devoted to maintain the BT technology- forecasts that around 70% of all the new cars will have a BT connectively by 2016; similarly, BT enabled mobile handsets will exceed 1.6 billion units by the end of 2015 (SIG, 2010).

Travel time (1) of a MAC-ID observed at time-synchronised BMS *zones* (*u* and *d*), can be directly obtained by matching the MAC-IDs and corresponding time stamp from the two *zones*.

$$TT(m,u,d) = T(m,d) - T(m,u) \quad (1)$$

Where:

TT(m,u,d) is the travel time from the *zone u* to the *zone d* for the device with MAC-ID = *m;*

T(m,k) is the time when the MAC-ID = m is observed at the k^{th} BMS zone.

The matched travel time data do contain noise due to reasons such as:

a) *Unknown mode*: Obtained travel time is for the BT device transported by a traveller utilising any mode (car, bus, bicycle, pedestrian etc.) of transport. Different modes have different travel time depending on their operational and behavioural characteristics. If one is interested in car travel time, then the presence of

pedestrians or bicycles can result in unrealistic high travel time values and vice-versa.

b) *No information outside the zone*: The estimate is only from the data available at *zones*, hence the actual travel pattern of the vehicle between the *zones* is unknown. A vehicle can rest along the route or can take a different route with significantly different travel time than that of the assumed route.

c) *Multiple matches*: Especially on arterial networks, a device can be observed at a *zone* and then it might take a detour, return to the same zone, and thereafter travel to the next *zone*. In such situations, a device can be observed twice at the first *zone* and only once at the second *zone*, resulting in two travel time values. Similarly, other combinations of multiple matches can occur, resulting in the noise.

d) *Missed observation*: A BT device has a probability of being discovered at a *zone* and not all devices passing the *zone* are discovered. For instance, say a device travels twice between zones *u* and *d.* During its first trips, the device was observed at *u* at time tu1, however it was missed at *d*. During its second trip, it was observed at *d* at time td2, but missed at *u*. Such observations will result in noisy travel time from *u* to *d* as (td2-tu1). Similarly, other combinations of observations can result in inaccurate travel time values.

In addition to the above, there are other issues related to the BMS data acquisition, which will be discussed later. In literature, filtering techniques, such as Moving Median Filter (Wang et al., 2011), Median Absolute Deviation (MAD) (Kieu et al., 2012), Box-and-Whisker filter (Tsubota et al., 2011) and other techniques utilising *Greensheld's model* and *least*

median of squares (Van Boxel et al., 2011) and *multiple matched filter* (Kieu et al., 2012) have been utilised to reduce noise from the directly matched travel time values.

Especially, on urban arterials, it is very challenging to estimate travel time from loops. Models have been proposed to estimate and predict travel time using traditional data sources on arterials (Bhaskar et al., 2011, Bhaskar et al., 2010, Bhaskar et al., 2009, Bhaskar et al., 2012, Kwong et al., 2009) and motorways (Zhang and Rice, 2003, van Lint et al., 2005, Sun et al., 1999, Soriguera and Robusté, 2011, Paterson and Rose, 2008, Li and Rose, 2011, Khosravi et al., 2011, Fei et al., 2011, Coifman and Krishnamurthy, 2007, Coifman and Kim, 2009). BMS data provides significant benefit to the road operators for estimating the travel time on road networks in a very cost effective manner. In literature, travel time from BMS data is compared with that from video cameras for motorways (Wang et al., 2011) and arterial (Mei et al., 2012) and promising results are reported.

For other studies (Haghani and Aliari, 2012), travel time obtained from traditional matching of BMS data is being considered as ground truth travel time. BT tracking is not only being explored for car travel times estimation, but also for other applications such as bicycle travel time (Mei et al., 2012), travel patterns of people movement in airports, shopping malls etc. (Bullock et al., 2010, Malinovskiy and Wang, 2012, O'Neill et al., 2006, Abedi et al., 2013), work zone delays (Haseman et al., 2010), Origin-Destination estimation (Barceló et al., 2012, Blogg et al., 2010, Barceló et al., 2010), route choice analysis (Hainen et al., 2011, Carpenter et al., 2012), and freeway travel time variability (Martchouk et al., 2011).

The amount of data collected from a BMS location depends on numerous factors related to the penetration of BT in the vehicles, software and hardware related with the Bluetooth protocol, etc. Researchers have experimented with the BMS antennae types, position and number against the quantity of data collected. A difference in the quantity of data collected by different antenna type, has been reported. Porter et al., (2011) recommends vertically polarized antennae with gain between 9 to 12 dBi. Vo et al., (2012) and Click and Lloyd (2012) reports that the use of more than one BMS at the site can increase the quantity of data collection.

As can be inferred from the above, literature is primarily focussed on the applications of direct match of BT MAC-ID's at different BMSs; there is limited fundamental understanding on the Bluetooth protocol based data acquisition process, and its impact on the accuracy and reliability of the analysis performed using the data. The objective of this paper is to fill this gap by modelling the theoretical properties of the BMS data and analysing the accuracy and reliability of travel time estimation using the data. To fulfill this objective, firstly the Bluetooth communication and data acquisition process is reviewed. Then, a framework for the proposed multi-layer simulation model, named *Traffic and Communication Simulation* (TCS), is presented. Finally, the results of the analysis performed using the TCS are discussed.

2 Bluetooth communication and data acquisition process

2.1 Bluetooth communication

Transport researchers and practitioners generally do not care about the theoretical details of the Bluetooth communication protocol. However, for better understanding of the accuracy and reliability of the data from BMS, in this section the relevant details are discussed.

Bluetooth is a short-range communication protocol, initially designed to replace cables connecting devices, which has been a success mainly due to its robustness, low power and low cost. The communication range between two Bluetooth devices depends on the power of the Bluetooth radio transmitter, sensitivity of the receiver, and the absorption rate of the medium. These devices are classified into three classes (Class-1, Class-2 and Class-3) as presented in Table 1. The communication ranges are the core specifications but the Bluetooth manufacturer has the flexibility to tune the range of the device as required. Murphy et al., (2002) have experimented with the communication range of Class-1 and Class-2 devices and have reported that both these classes outperformed the minimum range specification. Indeed, Class-1 and Class-2 were reported to be communicating at a maximum range of 250 m and 122 m, respectively.

Table 1 PLACE HERE

BMS is Class-1 type, and most of the portable devices, transported by the travellers (mobile phone, car navigation etc.), are Class-2 type. Given the communication range can be up to 250 m, which is beneficial for transport application as it can provide sufficient time for BMS

to discover the BT devices transported through the range. BMS can only read the MAC-ID and there is no information about the spatial distance between BMS and the respective BT device. The device can be anywhere within the range, resulting in a spatial error in the data being obtained by the BMS. The maximum error is equal to the communication distance.

Bluetooth operates in the unlicensed Industrial Scientific and Medical (ISM) band at 2.4 to 2.485 GHz. The ISM is shared by other wireless technologies such as Wifi, Near Field Communication (NFC), cordless phone etc. To avoid interference between the wireless devices sharing the ISM band and achieve an efficient transmission within the band, Bluetooth communication performs *Frequency Hopping*. In most countries, the ISM band is divided into 79 frequencies (channels) at intervals of 1 MHz. A Bluetooth device transmits and receives information by hopping over these channels. Devices communicating with each other (paired together) are synchronised so they are always hopping (changing) frequency in the same sequence, as determined by one of the devices (master device). The frequency hopping is at a rate of 1600 times per seconds (resulting in a time slot of 625 microseconds per channel). Thus, problems related to failing communication at a particular frequency due to fade or a particular interference is avoided, and both voice and data throughput during communication is improved. Researchers (Chen and Hung, 2011) have proposed analytical models to capture such *frequency hopping* behaviour.

A Bluetooth device (also termed as a Bluetooth unit) has two major states, being *standby* or *connection* state, and seven *modes* (or *sub-states*). *Standby* implies no interaction with the other devices and *connection* implies that data is being transferred. The seven *modes* are to

establish *connection*, and they are *inquiry*, *inquiry-scan, inquiry-response*, *page*, *page scan*, *slave-response* and *master-response*. Multiple devices can be connected, given one of them acts as a *Master* and the remaining as *Slaves.* The actual procedure for Bluetooth connection is complex, but can be simply modelled, as follows (*see* Figure 1):

i. The *Master* device has to be in *Inquiry mode* to inquire about the other devices (in *Inquiry-scan mode*) within the communication range by sending a package containing its information (address and clock).

ii. If the *Slave* is in *Inquiry-scan mode* then it scans the inquiry sent by *Master*. Thereafter, *Slave* can switch to *Inquiry-response mode* to respond, by sending its information (address and clock) for *Master*.

iii. *Master* listens to the response from the *Slave(s)* within its range and may switch to *Page mode* to page (hopping sequence and other information) the discovered *Slave* device(s).

iv. The *Slave* has to be in *Page-scan mode* to scan the page sent by *Master*, and may switch to *slave-response mode* to send its response (device access code).

v. Finally, the *Master* has to be in *Master-response mode* to send further information to establish final connection between the two.

BMS is only interested in the *inquiry* process of discovering the devices, where it (acting as a *Master*) should be able to acquire the MAC-IDs of the other devices (acting as *Slaves*) within its communication *zone*.

A device in a mode is transmitting and receiving information alternatively at a certain frequency defined for certain time slot, thereafter it hops to another frequency.

Information exchange should be in the same frequency, i.e. if *Master* sends its *inquiry* at frequency k, only those *Slaves*, which at that particular time instance are scanning at the same frequency k, could then scan this information. Moreover, in order to save power consumption, a unit in *inquiry–scan mode* only listens for a very short period of time (11.25 ms by default) and thereafter, enters *standby* state for a longer period of time (1.28 s). Hence, the discovery process (and connection process) is not instantaneous and requires time even in an ideal environment (where messages are not lost). Bluetooth protocol recommends a device to be in *inquiry* mode for 10.24 s (SIG, 2010). Indeed, Kasten and Langheinrich (2001) performed 1500 tests to establish distribution of the time needed for inquiry process and reported the probability of discovering a device in 1.910 s, 4.728 s and 5.449 s as 50%, 95% and 99%, respectively. Peterson et al. (2004, 2006) backed these results, where they have reported 99% of the devices can be discovered in 5.12 s.

Figure 1 PLACE HERE

2.2 BMS communication zone

The communication *zone* of the BMS depends on the type of antenna used (hardware). The *polarization* of an antenna (e.g., omnidirectional, directional) defines its communication coverage shape (horizontal and vertical), and the *gain* (strength, unit: dBi) of the antenna defines size of the coverage shape. Figure 2 illustrates two different communication zones: Figure 2*a* is for an omni-directional (or non-directional) antenna that transmits and receives signals from all directions equally well; Figure 2*b* is for a uni-directional antenna that maximises the signals along one direction and suppresses signals along other directions. Note: the shown *zones* are for illustration purpose only; the actual shape in the real environment is affected by the local installation factors such as attenuations and

reflections to the signals from trees, buildings etc. Depending on the usage, different antennae can be combined together to define the required shape and size of the communication *zone*.

The BMS range is the maximum distance from BMS, along a given direction, over which BMS can effectively communicate with BT devices. The communication range is directly proportional to the *gain* of the antenna. We have performed field experiments using antennae with different *gain* and have observed that 3 dBi, 9 dBi and 20 dBi antennae have around 35 m, 100 m and 150 m range, respectively. For traffic applications, range along the road section should be large enough to provide sufficient time for BMS to capture the MAC-IDs of the devices traversing through the zone. For this, generally a range of 100 m is preferred.

Figure 2 PLACE HERE

2.3 BMS data acquisition

The BMS is configured to be in continuous *inquiry* mode over a time-period termed as the *inquiry cycle (C_I)*, where BMS are alternatively sending the inquiry messages and scanning the potential replies over the range of predetermined frequency channels. These *cycles* are repeated as a seamless train of *inquiry cycles* for uninterrupted discovery of the devices. An inquiry train is illustrated in Figure 3*a*, where i^{th} inquiry starts at time t_{i-1} and ends at time t_i and C_I is the time difference between the two.

During an *inquiry* process, the device can be discovered at any time. In principle, BMS should be able to provide the exact time (within the *inquiry* process) of the discovery of the

MAC-ID. However, generally the data acquisition software linked with BMS only provides the MAC-IDs scanned during an *inquiry* but not the exact time when it is discovered. All the discovered MAC-IDs are linked to the time-stamp corresponding to the end (or start) of the respective *inquiry*. This is analogous to the inductive loop detectors used on road network. In principle, inductive loop detectors can provide exact time when the metal (vehicle) is detected. However, in-practice, loop detectors are configured to provide aggregated counts over the detection period (e.g. 30 s).

The aforementioned loss of exact time of detection contributes to the temporal error in the data acquisition. For instance, Figure 3*b* represents an example where during an i^{th} *inquiry*, a device is discovered at time t ($t_{i-1} \leq t < t_i$) and is reported at time t_i. Error in reporting the time when the device is discovered, is the difference of the time when the device is reported (t_i) and time when it is actually discovered (t).

Moreover, the exact location of the device within the zone is unknown and it can take time for the device to be discovered, once it has entered the BMS zone; this contributes to the temporal error in reporting the exact time when the device has entered or left the zone (further discussed and modelled in Section 3).

Figure 3 PLACE HERE

Note: Bluetooth communication is standardised (as discussed in Section 2.1). In principle, the concept of a BMS scanning process is the same for all the scanners. BMS follows the Bluetooth communication protocol and aims to capture the MAC-IDs of the discoverable devices (for which, only the *inquiry* process is required).

The aforementioned discussion is supported by the analysis performed on real data obtained from Brisbane, Australia. Brisbane is densely equipped with BMS locations – there are around 200 BMS locations on Brisbane arterials maintained by the Brisbane City Council and around 400 BMS locations are being targeted by the Department of Main Roads for motorways. Figure 4*a* represents one-day time series of the number of MAC-ID records observed in each second at a BMS location (an arterial intersection at Coronation drive, Brisbane). If all the observed MAC-IDs within the *inquiry cycle* are given the same time-stamp, then in this time series, one should expect positive values of MAC-ID observation only during the end of the *inquiry cycle*. Figure 4*b* represents the zoomed-in graph for Figure 4*a* where it can be seen that records are positive only during certain times and are zero in between. Here, we term *observation-gap* as the derivative of the time when the number of MAC-IDs reported is positive. *Observation-gap* should represent C_I or its multiple. We say 'multiple' because it can happen that during an *inquiry t*here is no observation and in such a case, the time difference between the time of two consecutive positive observations will be multiple of C_I. For the example shown in Figure 4*b* C_I = 14 s.

From Figure 4*a* it is observed that the maximum number of records for the site is 15 MAC-IDs per inquiry cycle. As expected, the numbers of observations are low from early morning until about 5 a.m. (time = $1.8 * 10^4$ s) and thereafter, increase during the day and finally drop off during the night.

An inquiry cycle can be configured to any reasonable value. Indeed, C_I for the BMS device for which the data is presented in Figure 4, is configured to 14 s. Although configured for a fixed C_I, the real data contains white noise. For instance, Figure 5*a* represents time series of the *observation gap* (C_I or its multiple) for the data presented in Figure 4. It can be seen that at times C_I is less than the configured 14 s value. The probability density for the *observation gap* is presented in Figure 5*b*, which shows peaks at configured C_I, and its multiples. The peaks at the multiple of C_I make sense because records are stored with time stamps that should be multiple of C_I.

Figure 4 PLACE HERE

Figure 5 PLACE HERE

2.4 Sample data from a BMS

In order to reduce the huge amount of data to be stored and transferred, data acquisition software generally reduces the data at the device level. For instance, in Brisbane, a record detected over consecutive *inquiry cycles* is stored only once with the timestamp corresponding to the time when it is first detected. Additionally, a field termed as *duration* is added to the data corresponding to the time difference between the first and last detection (*see* Table 2). For instance, in Table 2, *Device ID* 10 was detected for six consecutive inquiry cycles. Instead of storing the record six times with different time-stamps, the record is stored only once with duration of 84 s.

Table 2 PLACE HERE

3 Urban network travel time modelling from BMS data

Figure 6 illustrates time space diagram with the trajectory of a Bluetooth equipped vehicle, through the BMS communication zone and respective BMS *inquiry train* (shown in yellow). We use this figure as an example to define the following parameters needed for modelling the travel time from BMS data:

- A vehicle enters the BMS zone at time τ_A. It takes some time for a vehicle to be discovered by the BMS. It is first discovered at time τ_{fd} and its arrival time at zone is reported as τ'_A.
- The vehicle takes d (seconds) to travel within the zone, and during its stay within the zone it can be discovered multiple times by the BMS. Here d is the true actual *duration* of the vehicle.
- The vehicle actually departs from the zone at time τ_D (2). However, the vehicle was last discovered by BMS at time τ_{ld} (3) and its reported departure time is τ'_D.

$$\tau_D = \tau_A + d \tag{2}$$

$$\tau_{fd} \leq \tau_{ld} \leq \tau_D \tag{3}$$

- The reported duration of the vehicle (d') is related to τ'_A and τ'_D, as follows (4):

$$d' = \tau'_D - \tau'_A \tag{4}$$

- BMS is configured for a fixed C_I and ideally, it should not change with time. For this ideal condition, the value of d' (5) should be either multiple of C_I or zero.

$$d' = nC_I \tag{5}$$

Where: *n* is a natural number, the value for which is the number of additional *inquiry* cycles between τ'_A and τ'_D. For instance, in Figure 6, n = j – i. Note: if vehicle is observed only once, then n =0.

Considering the above, the temporal errors, ε_A (6) and ε_D (7), of the BMS in reporting the vehicles' arrival time and departure time from the zone, respectively is as follows:

$$\varepsilon_A = \tau'_A - \tau_A \quad (6)$$

$$\varepsilon_D = \tau_D - \tau'_D \quad (7)$$

Figure 6 PLACE HERE

On the arterial network, BMS is generally installed at the intersection. In Brisbane, BMS is installed in the signal controller box with its antenna drilled out of the box (*see* Figure 7). This is primarily due to practical reasons related to the uninterrupted supply of power for the BMS. Assuming BMS is at the signal controller near to the intersection, and depending on the delay observed at the signalised intersection, a vehicle can spend a significant time in the BMS zone. The travel profile of the vehicle within the BMS zone is non-uniform, i.e., stop-and-go running condition before the stop-line and accelerating or cruising beyond the stop-line. Therefore, to model the travel time, we define the following three sections that can have different travel time values (see Figure 8*a*):

- Section *Ex2Ex*: From the exit of the *u/s* BMS zone to the exit of *d/s* BMS zone;
- Section *S2S*: From the stop-line of the *u/s* intersection to the stop-line of the *d/s* intersection; and

- Section *En2En*: From the entrance of the *u/s* BMS zone to the entrance of the *d/s* BMS zone.

Figure 7: PLACE HERE

Figure 8: PLACE HERE

3.1 Section Ex2Ex: From the exit of the u/s BMS zone to the exit of the d/s BMS zone

The travel time for this section is mainly governed by the delay at the d/s intersection. Say TT_{Ex2Ex} (8) and TT'_{Ex2Ex} (9) represents the actual travel time and the estimated (from BMS) travel time for this section, respectively.

$$TT_{Ex2Ex} = \tau_{D,d/s} - \tau_{D,u/s} \tag{8}$$

$$TT'_{Ex2Ex} = \tau'_{D,d/s} - \tau'_{D,u/s} \tag{9}$$

Rearranging the above equations ((7), (8) and (9)) leads to the following relationship between the actual and the estimated travel time for this section:

$$TT_{Ex2Ex} = TT'_{Ex2Ex} + (\varepsilon_{D,d/s} - \varepsilon_{D,u/s}) \tag{10}$$

3.2 Section S2S: From the stop-line of the u/s intersection to the stop-line of the d/s intersection

Similar to the previous section, the travel time for this section is mainly governed by the delay at the d/s intersection, assuming there is no spillover from a further downstream link. Say TT_{S2S} (11)and TT'_{S2S} (12) represents the actual travel time and the estimated (from BMS) travel time for this section, respectively.

$$TT_{S2S} = TT_{Ex2Ex} + (\Delta_{u/s} - \Delta_{d/s}) \tag{11}$$

Where: $\Delta_{u/s}$ and $\Delta_{d/s}$ is the time needed to travel from the stop-line to the exit of the zone at the u/s intersection and the d/s intersection, respectively.

$$TT'_{S2S} = TT'_{Ex2Ex} + (\Delta'_{u/s} - \Delta'_{d/s}) \quad (12)$$

Where $\Delta'_{u/s}$ and $\Delta'_{d/s}$ is the estimated time needed to travel from the stop-line to the exit of the zone at the u/s intersection and the d/s intersection, respectively.

If u/s BMS and d/s BMS are at two consecutive signalised intersections, then TT_{S2S} is a good indicator for the d/s intersection performance where delay at the intersection is the difference between TT_{S2S} and the free-flow travel time of the section.

3.3 Section En2En: From the entrance of the u/s BMS zone to the entrance of the d/s BMS zone

The travel time for this section contains partial delays at both u/s and d/s intersections. Say TT_{En2En} (13) and TT'_{En2En} (14) represents the actual travel time and the estimated (from BMS) travel time for this section, respectively.

$$TT_{En2En} = \tau_{A,d/s} - \tau_{A,u/s} \quad (13)$$

$$TT'_{En2En} = \tau'_{A,d/s} - \tau'_{A,u/s} \quad (14)$$

Rearranging above equations ((6), (13) and(14)) leads to the following relationship between the actual and the estimated travel time for this section:

$$TT_{En2En} = TT'_{En2En} + (\varepsilon_{A,u/s} - \varepsilon_{A,d/s}) \quad (15)$$

4 Multi-layered Traffic and Communication Simulation (TCS) model

Here the aforementioned theory of BT communication and BMS data acquisition process is utilised to develop a multi-layered Traffic and Communication Simulation (TCS) model, where communication simulation is integrated with the microscopic traffic simulation.

Microscopic traffic simulation simulates the behaviour of vehicles on the road network, and can provide detailed vehicle trajectories. TCS randomly assigns the simulated vehicles with the BT, based on the configured penetration of the BT in the traffic stream. For instance, if we configure x% of traffic with Bluetooth, then, assuming each vehicle has an equal probability of being selected, x% of the simulated vehicles are randomly selected and assigned as BT equipped vehicles. The trajectories of BT equipped vehicles are input to the communication simulation, which simulates the BMS *inquiry* process and communicates with the BT equipped vehicles when they are within the BMS communication range (*see* Figure 9).

Figure 9: PLACE HERE

For TCS, an interface can be developed for integrating simulation packages, such as AIMSUN for traffic and OMNeT++ for communication simulation. For this research, we have utilised AIMSUN for traffic simulation and developed the communication simulation and the interface in Matlab. For communication simulation, the probability density of the time for discovering a Bluetooth device is adopted from the results from Kasten and Langheinrich (2001) where the probability of detecting the device within 1 s, 2 s, 3 s, 4 s and 5 s is 27.5%, 53%, 70.6%, 87%, 98.8%, and 99%, respectively.

A TCS model for a two lane arterial corridor has been developed, as shown in Figure 8*b*. Both upstream (u/s) and downstream (d/s) intersections are signalised. The distance between the two intersections is 1.1 km. At u/s intersection, traffic enters from all three directions, whereas, at d/s intersection, only through movement is considered. The BMS coverage area is indicated by the shaded region in the figure.

Traffic simulations have been performed for the following scenarios:

i. *Scenario U_U_C:* Both u/s and d/s intersections are under-saturated. The d/s signal is coordinated with the through movement at upstream. Hence, vehicles do not observe delay at d/s;
ii. *Scenario U_U_NC*: Both u/s and d/s intersections are under-saturated. The d/s signal is badly coordinated with the through movement at u/s, due to which, vehicles observe delay at both u/s and d/s intersections;
iii. *Scenario U_O*: The u/s intersection is under-saturated, the d/s intersection is over-saturated. Here, queues at d/s intersection are uncleared at the end of the signal cycle; and
iv. *Scenario O_O*: Both u/s and d/s intersections are over-saturated. Here, queues at both u/s and d/s intersections are uncleared at the end of the respective signal cycles.

For each of the aforementioned scenarios, ten replications are simulation. Each replication has different random seed, representing different vehicles' simulation. The following parameters are considered for the traffic simulation:

i. Speed limit of road is 60 km/hr;

ii. Stochastic vehicle (driver) speed limit acceptance factor (*f*) is normally distributed N(1.1, 0.1) and, $0.9 \leq f \leq 1.3$. The factor takes into account the difference in the compliance to the speed limit by different drivers. Here, the desired speed (speed at which the vehicle would like to be driving under free-flow conditions) of the simulated vehicle is *f* times the speed limit. For instance, f=1.1 for a simulated vehicle indicates that the desired speed of this vehicle is 10% higher than the speed limit of the road;

iii. Both intersections have signal cycle time of 90 s;

iv. Vehicles have stochastic acceleration rate (*a*), which is normally distributed N(3 m/s^2, 0.25 m/s^2) and , 2.5 m/s^2≤ a ≤ 3.5 m/s^2; and

v. Other parameters, such as length of the vehicle, and deceleration rates are also stochastic.

A pair of time-synchronised omni-directional BMS scanners with range of 100 m each are defined close to the u/s and d/s intersections, respectively. Communication simulation is performed for C_I ranging from 5 s to 60 s.

Referring to the indicated points in Figure 8*b*:

a) Exit-to-exit section is defined from point *B* to point *J;*

b) Stop-to-stop section is defined from points *E*, *G* and *F* to point *I*; and

c) Entrance-to-entrance section is defined from points *A*, *D* and *C* to point *H.*

Assuming that vehicles have equal probability of being equipped with Bluetooth, the data from the aforementioned simulations is utilised for the following discussions:

A) BMS data accuracy evaluation (Section 5): Here, we evaluate the accuracy of the BMS data for reporting the individual vehicle arrival and departure time from the BMS zone.

B) Accuracy and reliability of the travel time estimation for the aforementioned three sections (Section 6): Here, separate analysis is performed for individual vehicle travel time estimation and average travel time estimation:

    a. Individual vehicle travel time accuracy is evaluated in terms of its absolute magnitude (Sections 6.1.1, 6.2 and 6.3.1) and percentage (Sections 6.1.2, 6.2 and 6.3.2).

    b. Average travel time accuracy is evaluated (Sections 6.1.3, 6.2 and 6.3.3) for different penetration of Bluetooth in the traffic stream. Here, for each penetration rate we randomly select vehicles and repeat the process ten times with different values of the seed for random number generation. For instance, suppose a traffic simulation has 1000 vehicles, and we are interested in the average accuracy for the penetration rate of 3%. Then, we first randomly select 30 simulated vehicles as Bluetooth; perform communication simulation over these selected vehicles; and estimate the accuracy for different estimation periods. Thereafter, we repeat the process nine more times; and finally estimate the average from all these estimations.

5 BMS data accuracy evaluation

A Bluetooth equipped vehicle can arrive and depart from the BMS communication zone at any time. It is reported only after its arrival at the zone, hence temporal error of BMS in reporting the vehicle's arrival time (ε_A) is non-negative (16).

$$\varepsilon_A \geq 0 \tag{16}$$

Similarly, if the BT has communicated with BMS then the time at which it departs from the zone should not be less than the time when it has communicated. However, the time reported by BMS is the time corresponding to the end of the respective *inquiry* cycle that can be later than the time when the vehicle departs from the zone. This results in temporal error of the BMS in reporting the departure time (ε_D) as greater than or equal to $-C_I$ seconds (17).

$$\varepsilon_D \geq -C_I \tag{17}$$

We evaluate ε_A and ε_D for different values of C_I and the values are presented as a box-and-whisker plot in Figure 10. The bottom and top of the box represents 25th percentile (q_1) and 75th percentile (q_3), respectively. The band within the box is the median. The whiskers represent the data within ($q_3 + 1.5(q_3-q_1)$) and ($q_1 - 1.5(q_3-q_1)$). The red plus points represents the outliers, which are outside the whiskers. Analysing the values against different distribution functions, we conclude that the temporal error from BMS follows a *Generalised Gaussian Distribution* (GGD). The parameters of GGD (Location parameter (μ: Mean); Scale parameter (σ: Standard deviation) and Shape parameter (ν: Power index)) depend on C_I and the zone size, the results for which are present in Figure 11. If the expected value ([.]) for a distribution is defined by its mean, then from Figure 11*a*

it is clear that [ε_A] and [$|\varepsilon_D|$] are directly proportional to C_I. The scale parameter (Figure 11*b*) for the distribution also increases with C_I. The shape parameter (ν) equals 1, 2 and ∞ represents laplace, normal and uniform distributions, respectively. Figure 11*c* indicates that the temporal errors are more toward normal than uniform distribution.

Figure 10 PLACE HERE

Figure 11 PLACE HERE

6 Accuracy and reliability for travel time estimation from BMS data

The results of the analysis are reported separately for three sections (Exit to Exit, Entrance to Entrance and Stop-to-stop).

6.1 Analysis on the Exit-to-Exit travel time estimation

6.1.1 Absolute error in individual vehicle travel time estimation

Here, $Error_{Ex2Ex}$ represents the error in the estimation of the exit-to-exit individual vehicle travel, and is obtained by rearranging equation (10). The absolute error (18) is defined as follows:

$$\left|Error_{Ex2Ex}\right| = \left|TT_{Ex2Ex} - TT'_{Ex2Ex}\right| = \left|\varepsilon_{D,d/s} - \varepsilon_{D,u/s}\right| \quad (18)$$

The magnitude of error only depends on the BT communication within the BMS zones. It is independent of the time spent by the vehicle outside the zone. The longer the time spent by a BT equipped vehicle within the zone, the more likely it is detected by the BMS. Therefore, for the current analysis, we segregate the absolute error for individual vehicles (simulated from the scenarios: *U_U_C*, *U_U_NC*, *U_O*, and *O_O* as introduced in Section 4) into following four different cases based on the time a vehicle spends at the two zones:

a) Case-*LL*: Vehicle with lower *duration* (≤ 25 s) at both u/s and d/s BMSs. It includes vehicles that do not experience delay within the BMS zones.
b) *Case-LM*: Vehicle with lower *duration* at the u/s BMS but higher *duration* (>25 s) at the d/s BMS. It includes vehicles that experience delay only at the d/s BMS.
c) *Case-ML*: Vehicle with higher *duration* at the u/s BMS but lower *duration* at the d/s BMS. It includes vehicles that experience delay only at the u/s BMS.
d) *Case-MM*: Vehicle with higher *duration* at both u/s and d/s BMSs. It represents vehicles that experience delays at both u/s and d/s BMS.

Figure 12 represents the box-and-whisker plot for absolute errors versus C_I for the aforementioned four cases. It is observed that:

a) There is no significant difference in magnitudes of absolute error for the four cases. For lower C_I (less than 20 s), the 75^{th} percentile of the absolute error is less than 10 s for all the cases, and for higher C_I it can be around 25 s.
b) The median of the absolute error follows a cyclic pattern. The cycle peaks are different for different cases.
c) The maximum error increases with increase in C_I.

Figure 12 PLACE HERE

6.1.1.1 Discussion on the observed cyclic pattern

The aforementioned cyclic pattern is attributed to the error in estimation being the difference in temporal error of BMSs in reporting of the departure time at the upstream ($\varepsilon_{D,u/s}$) and downstream ($\varepsilon_{D,d/s}$), respectively. For certain combinations of C_I, individual vehicle $\varepsilon_{D,u/s}$ and $\varepsilon_{D,d/s}$ can balance each other, resulting in accurate estimation whereas, for other values it act in opposition, resulting in higher errors. If we plot $\varepsilon_{D,u/s}$ and $\varepsilon_{D,d/s}$ for each vehicle, then we can divide the plots into three regions as shown in Figure 13, where points close to the line of equality have perfect estimation, and the error in travel time estimation is proportional to its distance from the line of equality. The points left and right of the line of equality represents under-estimation and over-estimation of travel time, respectively. Figure 14 illustrates individual vehicle $\varepsilon_{D,u/s}$ and $\varepsilon_{D,d/s}$ corresponding to different values of C_I obtained from one of the simulation runs. In the current example, for C_I = 35 s, the points are close to the line of equality, resulting in higher accuracy in the individual vehicle travel time estimation, whereas for C_I = 31 s, the points are far from the line of equality resulting in higher error in the estimation.

Figure 13 PLACE HERE

Figure 14 PLACE HERE

To explore more deeply into the cyclic pattern, we consider an example with the following parameters (see Figure 15):

a) $C_{I,u/s}$ and $C_{I,d/s}$ as the *inquiry* cycle at the u/s BMS and the d/s BMS, respectively
b) Inquiry train at the d/s BMS has an offset of α (seconds) with respect to that at the u/s BMS i.e., the start of the *inquiry* at the d/s BMS is α seconds from that of the u/s BMS

c) Exit-to-exit travel time for a vehicle from the u/s BMS to the d/s BMS is T_{exit}

d) For the simplicity of explanation, assume that the time when the vehicle is last discovered at the BMS zone is equal to the time when it has departed from the zone

e) Time when the vehicle is reported at the u/s BMS and the d/s BMS equals $nC_{I,u/s}$ and $mC_{I,d/s} + \alpha$, respectively (where n and m are natural numbers; and $mC_{I,d/s} + \alpha$ is greater than nC_I)

Figure 15 PLACE HERE

Here, temporal error of BMSs in reporting the departure time at upstream ($\varepsilon_{D,u/s}$) and downstream ($\varepsilon_{D,d/s}$), respectively is given as:

$$\varepsilon_{D,d/s} = mC_{I,d/s} + \alpha - (t_o + T_{exit}) \tag{19}$$

$$\varepsilon_{D,u/s} = nC_{I,u/s} - t_o \tag{20}$$

Exit to exit travel time estimation for this vehicle is perfect, if $\varepsilon_{D,u/s}$ and $\varepsilon_{D,d/s}$ are equal. If so, then the following equation (21) implies:

$$\begin{aligned} &\varepsilon_{D,u/s} = \varepsilon_{D,d/s} \\ &\Rightarrow nC_{I,u/s} - t_o = mC_{I,d/s} + \alpha - (t_o + T_{exit}) \\ &\Rightarrow T_{exit} - \alpha = mC_{I,d/s} - nC_{I,u/s} \end{aligned} \tag{21}$$

Relationship (22) between travel time of the vehicle (T_{exit}), inquiry train offset (α) and scan cycle (C_I) can be obtained by rearranging the above equation (21), and assuming $C_{I,u/s}$ and $C_{I,d/s}$ are equal.

$$\begin{aligned} &if \;\; C_{I,u/s} = C_{I,d/s} = C_I \\ &\qquad T_{exit} - \alpha = (m-n)C_I \end{aligned} \tag{22}$$

Where: m and n are natural numbers.

This indicates that vehicles, having travel time as multiple of C_I plus a constant (α) should have perfect estimation of exit-to-exit travel time from the BMSs data. This explains the reasons why certain values of C_I results in higher accuracy, and hence the cyclic pattern in accuracy estimation.

To further support this argument, we perform simulation on a free-flow network (through traffic only and without considering signals). Here, there is no congestion on the road network, and the difference in the individual vehicle travel time is due to the difference in the individual driver speed limit acceptance factor (f). Three different traffic simulations are performed with the speed limit of 40 km/hr, 60 km/hr and 80 km/hr, respectively. The travel time distributions for the three simulations are presented (as box-and-whisker plots) in the Figure 16. We define t_{40}, t_{60} and t_{80} as the average observed travel time for the speed limit of 40 km/hr, 60 km/hr and 80 km/hr, respectively (See Figure 16: $t_{40} \approx 104$ s, $t_{60} \approx 67$ s, and $t_{80} \approx 50$ s). For communication simulation, the offset (α) is zero seconds. Mean Absolute Error (MAE_{Ex2Ex}) (23) in travel time estimation from the BMSs data is independently estimated for different TCS simulations (traffic simulations over the aforementioned speed limits and communication simulations over C_I).

$$MAE_{Ex2Ex} = \frac{\sum_{i=1 to N} \left| TT_{Ex2Ex,i} - TT'_{Ex2Ex,i} \right|}{N} \quad (23)$$

Where: *N* is the number of simulated vehicles for which the error is estimated.

The results are presented in Figure 17. One can see that the MAE_{Ex2Ex} has a cyclic pattern, the local minima for which is different for different speed limit cases. For instance, for speed limit of 40 km/hr (green triangles in the figure), MAE_{Ex2Ex} drops for $C_I \approx \frac{t_{40}}{2}, \frac{t_{40}}{3}, \frac{t_{40}}{4}$.

Figure 16 PLACE HERE

Figure 17 PLACE HERE

6.1.2 Accuracy and reliability of individual vehicle travel time as percentage of actual travel time

The magnitude of the absolute error, as presented in the last section, does not depend on the congestion level (all the four cases are the same). However, the travel time between the two BMS zones directly depends on the distance between the zones and the level of congestion on the link joining the zones. This indicates that if we estimate error as a percentage of travel time, then shorter links will have more percentage error than larger links; and congested regions will have lower percentage error than non-congested region.

For the current analysis, the link joining the u/s and d/s BMS intersections is 1.1 km. For a given C_I, we define the accuracy (25) and reliability (27) in travel time estimation as follows:

$$MAPE_{Ex2Ex} = \frac{\sum_{i=1 to N} \left(\frac{\left|TT_{Ex2Ex,i} - TT'_{Ex2Ex,i}\right|}{TT_{Ex2Ex,i}}\right)}{N} \quad (24)$$

$$Accuracy_{Ex2Ex} = (1 - MAPE_{Ex2Ex}) \quad (25)$$

$$STDEV_{Ex2Ex}(\%) = \sqrt{\frac{(TT_{Ex2Ex,i} - TT'_{Ex2Ex,i} - MAE)^2}{N-1}} \quad (26)$$

$$\text{Reliability}_{Ex2Ex} = \frac{1}{STDEV_{Ex2Ex}} \quad (27)$$

Where:

$TT_{Ex2Ex,i}$ is the exit-to-exit individual vehicle travel time for the i^{th} individual vehicle

N is the number of vehicles

MAPE is Mean Absolute Percentage Error

STDEV is the standard deviation of the error in the estimation of individual vehicle travel time; Reliability is defined as the inverse of the standard deviation.

Green triangles in Figure 18*a* and Figure 18*b* represent the results for accuracy of individual vehicles for exit-to-exit travel time estimation for under-saturated and over-saturated traffic conditions, respectively. Similarly, green triangles in Figure 19*a* and Figure 19*b* represent the results for reliability of individual vehicles for exit-to-exit travel time estimation for under-saturated and over-saturated traffic conditions, respectively. As expected, both accuracy and reliability have a decreasing trend with C_I. The actual pattern is cyclic where accuracy increases for a range of C_I and thereafter starts decreasing and so on. This is due to the same reasons as discussed in Section 6.1.1.1. The accuracy and reliability for over-saturated traffic conditions are better than that of under-saturated traffic conditions. The results presented are for a link with 1.1 km in length. For shorter links, say 550 m, the accuracy will be further lowered- the percentage errors should be twice that of 1.1 km long link (further discussed in Section 7).

Figure 18 PLACE HERE

Figure 19 PLACE HERE

6.1.3 Accuracy and reliability of average travel time estimation

In section 6.1.1, we presented the results for the absolute error in individual vehicle, travel time estimation. Analysing the distribution of the magnitude of the error (see Figure 20) in the estimation of the individual vehicle travel time for all the vehicles, we observe that the median (and mean) is close to zero. This indicates that if all the vehicles are equipped with Bluetooth, then average travel time from the Bluetooth data should be accurate because the errors from different vehicles can balance each other. However, not all the vehicles are equipped with Bluetooth, and in this section we compare the accuracy of average travel time estimation from BMS under different BT penetration rate. For the current analysis, the average is over periods of 6 minutes (Δt) each.

Figure 20 PLACE HERE

Traffic simulation provides actual travel time values for all the vehicles. Say, during an estimation time window (Δt), there are n_a numbers of individual vehicle travel time points obtained from all the vehicles travelling during the same time window. We define $AvgTT_{A,\Delta t}$ (28) as actual average travel time from these n_a vehicles.

$$AvgTT_{A,\Delta t} = \frac{\sum_{i=1}^{n_a} TT_{Ex2Ex,i}}{n_a} \quad (28)$$

Not all the vehicles are equipped with Bluetooth. Hence, simulating BMS data only provides n_b number of travel time points during the Δt time period. We define $AvgTT_{B,\Delta t}$ (29) as the estimated (from BMSs) average travel time from these n_b vehicles.

$$AvgTT_{B,\Delta t} = \frac{\sum_{i=1}^{n_b} TT'_{Ex2Ex,i}}{n_b} \quad (29)$$

The estimated average travel time from BMSs data is compared with that from the actual average travel time and we define $APE_{\Delta t}$ (30) as the absolute percentage error in average travel time estimation during Δt time period

$$APE_{\Delta t} = \frac{\left| AvgTT_{A,\Delta t} - AvgTT_{B,\Delta t} \right|}{AvgTT_{A,\Delta t}} \quad (30)$$

Finally, the accuracy ($A_{\Delta t}$) for the average travel time estimation from different estimation periods (Δt =1 to T) is defined in equation (31): Note: three hours of simulation, with 10 replications each, and 10 times selection of Bluetooth vehicles each, will have 3*10*10*10 (=T) time windows of 6 minutes each.

$$A_{\Delta t} = 1 - \frac{\sum_{\Delta t=1}^{T} APE_{\Delta t}}{T} \quad (31)$$

Here, we also define another indicator for accuracy as $A5_{\Delta t}$ (32) which is the 5th percentile of the average accuracy obtained during different simulation runs. It means that 95% of the times the observed accuracy is more than $A5_{\Delta t}$ value. Hence, $A_{\Delta t}$ indicates the average performance whereas, $A5_{\Delta t}$ indicates the confidence in the accuracy.

$$A5_{\Delta t} = 1 - 95th\ percentile\ of\ APE_{\Delta t}\big|_{\Delta t=1\ to\ T} \quad (32)$$

The results presented here are for C_I = 20 s. Green triangles in Figure 21, Figure 22 and Figure 23 illustrate results for $A_{\Delta t}$, $A5_{\Delta t}$ and reliability versus different Bluetooth penetration rate, respectively for both under-saturated and over-saturated traffic

conditions. Here, reliability is defined (similar to equation (27)) as the inverse of the standard deviation of the error in the estimation of average travel time. It can be seen that both the defined accuracies increase with increase in the penetration rate. For lower penetration rate (< 5%) there is significant marginal improvement in accuracy if penetration rate is increased. However, for higher penetration rate the marginal increase is not that significant. For the current analysis $A_{\Delta t}$ and $A5_{\Delta t}$ are more than 90% and 80% respectively, for non-zero penetration rate. Reliability of the estimation also increases (see Figure 23) with the increase in the penetration rate.

Figure 21 PLACE HERE

Figure 22 PLACE HERE

Figure 23 PLACE HERE

Comparing these results with the individual vehicle accuracy obtained earlier (Figure 18), for C_I = 20 s, indications are that average travel time estimation performance is better than individual vehicle travel time obtained from the BMS data. For instance:

a) Refer to Figure 21, for penetration rate more than 5%, observed accuracies are more than 96% and 97.5% for under-saturated over-saturated traffic, respectively.
b) Refer to Figure 18, for C_I equals 20 s, observed accuracies are equal to 85% and 94.5% for under-saturated over-saturated traffic, respectively.

This confirms that the temporal errors in the travel time estimation from different vehicles can indeed balance each other, when considering average travel time, resulting in better accuracy from average travel time than that of individual vehicles.

6.2 Analysis on the Stop-to-Stop travel time estimation

Stop-to-stop individual vehicle travel time (TT_{S2S}) is defined by equation (11), which is obtained from TT_{Ex2Ex} and respective time needed to travel from stop-line to the exit of the zone at u/s intersection ($\Delta_{u/s}$) and d/s intersection ($\Delta_{d/s}$), respectively. Here $\Delta_{u/s}$ and $\Delta_{d/s}$ depends on the speed of the vehicle within the BMS zone, once it has crossed the stop-line. For instance, for through traffic in Figure 8*b*: $\Delta_{u/s}$ is the travel time of the vehicle from point *G* to point *B;* and $\Delta_{d/s}$ is vehicle travel time from point *I* to point *J*.

The value of Δ depends on various factors such as:

A) The initial speed of the vehicle at the stop-link (*u*);

B) Vehicle acceleration rate (*a*);

C) Maximum desired speed of the vehicle (=f.v; where *v* is the speed limit of the road, and *f* is the speed limit acceptance factor). Note: a vehicles' initial speed at the stop-line is not greater than its maximum desired speed (u ≤ f.v);

D) Size of the BMS zone (say distance from stop-line to zone exit is *r*); and

E) Traffic conditions on the downstream link.

Assuming there is no spillover at the downstream link. By applying simple physics, one can easily establish the equation for Δ (33) as follows:

$$\Delta = \begin{cases} \dfrac{f.v-u}{a} + \dfrac{r-s}{f.v} & if\ r > s \\ \dfrac{-u+\sqrt{u^2+2.a.r}}{a} & if\ r \le s \end{cases} \qquad (33)$$

$$where: s = \frac{(f.v)^2 - u^2}{2.a}$$

Figure 24 provides values of Δ for v= 60 km/hr; r = 100 m; a =[2.5 m/s^2, 3 m/s^2 , 3.5 m/s^2]; and f = 1 (i.e., vehicle will drive at the speed limit and will not exceed it). One can see that Δ varies from 6 s to 9.5 s, for the defined parameters. The first vehicle in queue at the stop-line has to accelerate from zero and hence has higher Δ than the one that enters the intersection with higher speed.

Figure 24 PLACE HERE

BMS data neither provides speed of the vehicle at the stop-line nor its acceleration rate. Hence, practically it is not possible to estimate Δ from BMS data using an equation (33). As discussed earlier (*Refer to* Section 2.4), BMS data does provides *duration* (time needed by a vehicle to travel through the BMS zone). Thus, for the current analysis, we explore the relationship between *duration* and Δ with the aim to estimate Δ from *duration*.

Figure 25 represents such a relationship obtained from the simulation of individual vehicles for a BMS zone of 100 metre radius. Here *duration* is the true *duration* (*d*) of the vehicle. It is observed that as *duration* increases, the ratio of Δ and *duration* decreases. Note: low duration of 10 s corresponds to the vehicles travelling at around 71 km/hr (17% higher than the speed limit) during non-congested conditions (Refer to the simulation parameters defined in Section 4).

We propose the following functional relationship (34) between duration and Δ:

$$\frac{\Delta}{d} = \frac{a}{d^b} \quad (34)$$
$$\Rightarrow \Delta = a * d^{(1-b)}$$

Where: *a* and *b* are calibration parameters that depends on the zone size and speed limit of the road.

The data presented from Figure 25*b* is utilised to calibrate the above equation; the obtained parameters are: *a*= 8.2624 and *b* = 0.978 with R^2 = 99.4%.

The above explanation is with actual duration (d) of the vehicles, which is the ideal condition. As discussed earlier the data provided by BMS is estimated duration (d'). Refer to Figure 6, actual (*d*) and estimated (*d'*) durations are related as follows:

$$d = d' + \varepsilon_A + \varepsilon_D \tag{35}$$

From equations (16), (17) and (35) it can be shown that (d-d') ≥-C_I. Figure 26 represents the relationship between *d* and *d'* for the simulated results presented in Figure 25. Here, C_I = 20 s, as expected (*see* equation (5)) observed *d'* (=0 s, 20 s, 40 s and 60 s) is multiples of C_I. Zero value of *d'* indicates that the vehicle is detected only once by BMS. Ideally, vehicle should have a minimum duration that corresponds to the free-flow travel time of the vehicle. Here, free-flow duration is around 10 s and the first positive *d'* is 20 s. Therefore, we replace 0 s duration with 15 s (mean of 10 s and 20 s) and represent the relationship between duration and Δ in Figure 27, where red stars correspond to the estimated duration and blue diamonds correspond to the actual duration. In the absence of any further information, we do not perform any adjustment to the observed 20 s, 40 s and 60 s duration.

Replacing *d* with *d'* in equation (34) we can define Δ' (an estimate for Δ for a given value of estimated duration) using the aforementioned calibration values:

$$\Delta^{'} = 8.2624 * d^{'(1-0.978)} \quad (36)$$

Figure 28 illustrates the box-and-whisker plot for the error in estimation of Δ (=Δ- Δ') for different values of *d'*. It can be seen that most of the errors are within ±0.5 s, though the error range between [-2.5, 2.5] seconds.

Applying the above model(36) to estimate $\Delta_{u/s}$ and $\Delta_{d/s}$ for different scenarios (discussed in Section 4), we evaluate the performance of stop-to-stop travel time estimation. As expected, the performance of the TT_{S2S} is similar to that of TT_{Ex2EX}, which is illustrated with the simulation results presented as blue diamonds in Figure 18, Figure 19, Figure 21, Figure 22, and Figure 23. These points are close to exit-to-exit results (blue triangles). The results indicate that in the absence of the *d*, the *d'* can be used for estimating Δ and defining stop-to-stop travel time.

Figure 25 PLACE HERE

Figure 26 PLACE HERE

Figure 27 PLACE HERE

Figure 28 PLACE HERE

6.3 Analysis on the Entrance-to-Entrance travel time estimation

In this section, we analyse the performance of entrance-to-entrance travel time estimation. The procedure for the analysis is similar to section 6.1 for exit-to-exit travel time. The

equations (24) to (32) are used to define the accuracy and reliability, with respective consideration of entrance-to-entrance travel time instead of exit-to-exit travel time.

6.3.1 Absolute error in individual vehicle travel time estimation

Here, we estimate absolute error for entrance-to-entrance travel time estimation by rearranging equation (15) as follows:

$$\left|Error_{En2En}\right| = \left|TT_{En2En} - TT'_{En2En}\right| = \left|\varepsilon_{A,u/s} - \varepsilon_{A,d/s}\right| \quad (37)$$

Figure 29, represents the box-and-whisker plot for absolute errors from entrance-to-entrance travel time versus C_I for the aforementioned four cases (*case-LL*, *case-LM*, *case-ML* and *case-MM*). It is observed that the median and 75th percentile of the absolute error for entrance-to-entrance travel time with respect to C_I is similar to that of exit-to-exit travel time (Figure 12). However, the outliers are of a much larger value compared to that of entrance-to-entrance. This can be attributed to the fact that errors in entrance-to-entrance travel time and exit-to-exit travel time are defined by ε_A and ε_D, respectively, with ε_A in general being greater than ε_D (Refer to Figure 10 and Figure 11*a*).

Similar to the previous cases, the accuracy and reliability of an individual vehicle with respect to the C_I is cyclic pattern. This is due to the same reasons as discussed in section 6.1.1. For instance, Figure 30 represents $\varepsilon_{A,u/s}$ and $\varepsilon_{A,d/s}$ from a simulation run for different C_I where for C_I = 35 s the points are close to the line of equality ($\varepsilon_{A,u/s}$ and $\varepsilon_{A,d/s}$ can balance each other). For C_I = 54 s the points are far from the line of equality, resulting in quite considerable error.

Figure 29 PLACE HERE

Figure 30 PLACE HERE

6.3.2 Accuracy and reliability of individual vehicle travel time as percentage of actual travel time

If we consider the accuracy and reliability with respect to the percentage of travel time as defined in Section 6.1.2, the red rectangles in Figure 18 and Figure 19 represent the accuracy and reliability for individual vehicle entrance-to-entrance travel time. It is observed that in general, entrance-to-entrance provides slightly better accuracy (%) for an individual vehicle as compared to that of the previous exit-to-exit and stop-to-stop sections. However, there is not much difference in the absolute error for individual vehicle travel time obtained from exit-to-exit or entrance-to-entrance. Entrance-to-entrance travel time contains delay from both upstream and downstream intersections, resulting in higher actual travel time compared to that of exit-to-exit. Because of this, the percentage error with respect to actual travel time is lower, resulting in a higher degree of accuracy.

6.3.3 Accuracy and reliability of average travel time estimation

The red rectangles in Figure 21, Figure 22 and Figure 23 represent the $A_{\Delta t}$, $A5_{\Delta t}$, and reliability for average travel time estimation. Contrary to the individual vehicle travel time accuracy, the accuracy for average travel time is lower than that of exit-to-exit and stop-to-stop sections. This is mainly because the entrance-to-entrance section travel time includes partial delays from both upstream and downstream intersections, and has significantly larger variation in travel time than that compared to the exit-to-exit section. If the travel time variation is large, then statistically we need a greater sample size for a better estimation of the average.

7 Discussion on the travel time estimation accuracy and distance between BMS scanners

The analysis performed above clearly indicates that the magnitude of the errors in the travel time estimation from BMS data is due to the technical limitations of BMS and its communication with the in-vehicle Bluetooth. The error is independent of the travel of the vehicle outside the zone. Hence, percentage error in travel time estimation from BMS should be higher for shorter links or sections with higher speed-limits (such as motorway). Figure 31 illustrates results from a simulation performed on study sections with lengths varying from 500 m to 5 km, and average speed of the section varying from 10 km/hr to 50 km/hr. It can be seen that the percentage error in the travel time estimation decreases with increase in the distance between the BMS scanners. Similarly, for a given section, percentage error in the travel time estimation decreases with the decrease in average travel speed (increase in travel time) along the section.

Having said that, if the distance between the scanners is increased, then especially on urban arterials it will raise other concerns such as:

A) Estimated travel time can be from vehicles that travel an alternate route to that of the assumed corridor between the BMS locations. This can result in significant noise in travel time values.

B) Lower matching of MAC-IDs between the u/s BMS and the d/s BMS, due to significant mid-section sink and sources (such as, side streets, on/off ramps). This can result in lower sample size of estimated travel time and corresponding lower confidence in average travel time estimation.

Further research is recommended, in order to analyse the optional distance between BMS scanners for traffic information.

Figure 31 PLACE HERE

8 Conclusions and future research directions

BMS is one of the cheapest sources of data and has the potential for providing rich information for area-wide traffic monitoring such as "live reporting" of the travel activity of the road users who carry BT-equipped devices. For better understanding of the data, it is important to identify and quantify the errors in the data.

After matching and filtering the BT data points, a good graphical representation of travel time patterns can be easily visualised. However, utilising the travel time estimates for real time applications such as signal control and traveller information system, should consider the accuracy and reliability of the estimates.

In this paper, a framework to model the traffic and communication simulation is proposed (TCS model). The TCS model is first utilised to evaluate the modelled temporal errors from the BMS data and thereafter, the accuracy and reliability of travel time estimations from BMS data are analysed. Following are the key findings:

a) It is observed that the temporal error in BMS follows Generalised Gaussian Distribution, the parameters for which are the function of the inquiry cycle (C_I) of the BMS.

b) Individual vehicle travel time accuracy follows a cyclic pattern as a function of C_I, the reason for which are analysed thoroughly.

c) It is observed that the temporal error in the travel time estimation from different vehicles can indeed balance each other, resulting in better accuracy from average travel time than that of individual vehicles.

d) The magnitude of error in travel time from BMS data depends on the communication of the BMS with the Bluetooth within the BMS zone, and is independent of the travel between the BMS zones. Hence, as the distance between the BMS scanner increases, or speed along the corridor decrease, the percentage error in the travel time estimation decreases.

Depending on the modelled section on signalised urban corridor, three different models (Exit-to-exit, Stop-to-Stop and Entrance-to-Entrance) for travel time estimation are proposed.

e) Entrance-to-Entrance includes a portion of delay observed at the upstream intersection. Hence, it is recommended that for utilising the travel time estimates from Bluetooth for ITS applications such as signal control optimisation, Exit-to-exit (or Stop-to-Stop) should be used.

f) A model to estimate Stop-to-Stop from Exit-to-exit is proposed, where duration data from BMS zones is effectively utilised.

The proposed TCS framework has shown promising results. The framework is currently being utilised for understanding crowd monitoring utilising Bluetooth and Wifi data.

Following are the recommended future research directions:

a) Theoretically explore the relationship between measured BMS duration, actual vehicle duration and signal performance.
b) Analyse the optimal distance between the BMS scanner locations for traffic applications.

Acknowledgements

We acknowledge the partners of the Smart Transport Research Centre, Brisbane City Council and Queensland University of Technology for their support to this research. We also gratefully acknowledge the anonymous referees for their constructive comments and suggestions.

References

ABEDI, N., BHASKAR, A. & CHUNG, E. Bluetooth and Wi-Fi MAC Address Based Crowd Data Collection and Monitoring: Benefits, Challenges and Enhancement. 36th Australasian Transport Research Forum (ATRF), 2 - 4 October 2013 Brisbane, Australia.

BARCELÓ, J., MONTERO, L., BULLEJOS, M., SERCH, O. & CARMONA, C. A Kalman Filter Approach for the Estimation of Time Dependent OD Matrices Exploiting Bluetooth Traffic Data Collection. Transportation Research Board 91st Annual Meeting 2012.

BARCELÓ, J., MONTERO, L., MARQUÉS, L. & CARMONA, C. 2010. Travel Time Forecasting and Dynamic Origin-Destination Estimation for Freeways Based on Bluetooth Traffic Monitoring. *Transportation Research Record: Journal of the Transportation Research Board,* 2175**,** 19-27.

BHASKAR, A., CHUNG, E. & DUMONT, A.-G. 2009. Estimation of Travel Time on Urban Networks with Midlink Sources and Sinks. *Transportation Research Record: Journal of the Transportation Research Board,* 2121**,** 41-54.

BHASKAR, A., CHUNG, E. & DUMONT, A.-G. 2010. Analysis for the Use of Cumulative Plots for Travel Time Estimation on Signalized Network. *International Journal of Intelligent Transportation Systems Research,* 8**,** 151-163.

BHASKAR, A., CHUNG, E. & DUMONT, A.-G. 2011. Fusing Loop Detector and Probe Vehicle Data to Estimate Travel Time Statistics on Signalized Urban Networks. *Computer-Aided Civil and Infrastructure Engineering,* 26**,** 433-450.

BHASKAR, A., CHUNG, E. & DUMONT, A.-G. 2012. Average Travel Time Estimations for Urban Routes That Consider Exit Turning Movements. *Transportation Research Record: Journal of the Transportation Research Board,* 2308**,** 47-60.

BLOGG, M., SEMLER, C., HINGORANI, M. & TROUTBECK, R. Travel time and origin-destination data collection using Bluetooth MAC address readers. 33rd Australasian Transport Research Forum, 2010 Canberra, Australia.

BULLOCK, D. M., HASEMAN, R., WASSON, J. S. & SPITLER, R. Anonymous Bluetooth Probes for Airport Security Line Service Time Measurement: The Indianapolis Pilot Deployment. 89th Annual Meeting in Transportation Research Board, 2010 Washington, DC, USA.

CARPENTER, C., FOWLER, M. & ADLER, T. J. 2012. Generating Route Specific Origin-Destination Tables Using Bluetooth Technology. *Transportation Research Board 91st Annual Meeting*

CHEN, L.-J. & HUNG, H.-H. 2011. A Two-State Markov-Based Wireless Error Model for Bluetooth Networks. *Wireless Personal Communications,* 58**,** 657-668.

CLICK, S. M. & LLOYD, T. Applicability of Bluetooth Data Collection Methods for Collecting Traffic Operations Data on Rural Freeways. Transportation Research Board 91st Annual Meeting 2012.

COIFMAN, B. & KIM, S. 2009. Speed estimation and length based vehicle classification from freeway single-loop detectors. *Transportation Research Part C: Emerging Technologies,* 17**,** 349-364.

COIFMAN, B. & KRISHNAMURTHY, S. 2007. Vehicle reidentification and travel time measurement across freeway junctions using the existing detector infrastructure. *Transportation Research Part C: Emerging Technologies,* 15**,** 135-153.

FEI, X., LU, C.-C. & LIU, K. 2011. A bayesian dynamic linear model approach for real-time short-term freeway travel time prediction. *Transportation Research Part C: Emerging Technologies,* 19**,** 1306–1318.

HAGHANI, A. & ALIARI, Y. 2012. Using Bluetooth sensor data for ground-truth testing of reported travel times. *Transportation Research Board 91st Annual Meeting.* Washington D.C., USA.

HAINEN, A., WASSON, J., HUBBARD, S., REMIAS, S., FARNSWORTH, G. & BULLOCK, D. 2011. Estimating Route Choice and Travel Time Reliability with Field Observations of Bluetooth Probe Vehicles. *Transportation Research Record: Journal of the Transportation Research Board,* 2256**,** 43-50.

HASEMAN, R., WASSON, J. & BULLOCK, D. 2010. Real-Time Measurement of Travel Time Delay in Work Zones and Evaluation Metrics Using Bluetooth Probe Tracking. *Transportation Research Record: Journal of the Transportation Research Board,* 2169**,** 40-53.

KASTEN, O. & LANGHEINRICH, M. 2001. First Experiences with Bluetooth in the Smart-Its Distributed Sensor Network. *Workshop on Ubiquitous Computing and Communications PACT 2001.* Barcelona, Spain.

KHOSRAVI, A., MAZLOUMI, E., NAHAVANDI, S., CREIGHTON, D. & VAN LINT, J. W. C. 2011. A genetic algorithm-based method for improving quality of travel time prediction intervals. *Transportation Research Part C: Emerging Technologies*.

KIEU, L. M., BHASKAR, A. & CHUNG, E. 2012. Bus and car travel time on urban networks: Integrating Bluetooth and Bus Vehicle Identification Data. *25th Australian Road Research Board Conference.* Perth, Australia.

KWONG, K., KAVALER, R., RAJAGOPAL, R. & VARAIYA, P. 2009. Arterial travel time estimation based on vehicle re-identification using wireless magnetic sensors. *Transportation Research Part C: Emerging Technologies,* 17**,** 586-606.

LI, R. & ROSE, G. 2011. Incorporating uncertainty into short-term travel time predictions. *Transportation Research Part C: Emerging Technologies,* 19**,** 1006-1018.

MALINOVSKIY, Y. & WANG, Y. Pedestrian Travel Pattern Discovery Using Mobile Bluetooth Sensors. Transportation Research Board 91st Annual Meeting 2012.

MARTCHOUK, M., MANNERING, F. & BULLOCK, D. 2011. Analysis of Freeway Travel Time Variability Using Bluetooth Detection. *Journal of Transportation Engineering,* 137**,** 697-704.

MEI, Z., WANG, D. & CHEN, J. 2012. Investigation with Bluetooth Sensors of Bicycle Travel Time Estimation on a Short Corridor. *International Journal of Distributed Sensor Networks,* 2012.

MURPHY, P., WELSH, E. & FRANTZ, J. P. Using Bluetooth for Short-Term Ad-Hoc Connections Between Moving Vehicles: A Feasibility Study. IEEE Vehicular Technology Conference 2002 2002 Birmingham, AL. 414-418.

NUSSER, R. & PELZ, R. M. Bluetooth-based wireless connectivity in an automotive environment. Vehicular Technology Conference, 2000. IEEE VTS-Fall VTC 2000. 52nd, 2000 2000. 1935-1942 vol.4.

O'NEILL, E., KOSTAKOS, V., KINDBERG, T., SCHIEK, A., PENN, A., FRASER, D. & JONES, T. 2006. Instrumenting the City: Developing Methods for Observing and Understanding the Digital Cityscape *In:* DOURISH, P. & FRIDAY, A. (eds.). Springer Berlin / Heidelberg.

PASOLINI, G. & VERDONE, R. Bluetooth for ITS? Wireless Personal Multimedia Communications, 2002. The 5th International Symposium on, 27-30 Oct. 2002 2002. 315-319 vol.1.

PATERSON, D. & ROSE, G. 2008. A recursive, cell processing model for predicting freeway travel times. *Transportation Research Part C: Emerging Technologies,* 16**,** 432-453.

PETERSON, B. S., BALDWIN, R. O. & KHAROUFEH, J. P. 2004. A Specification-Compatible Bluetooth Inquiry Simplification. *37th Hawaii International Conference on System Sciences.* Big Island, Hawaii

PETERSON, B. S., BALDWIN, R. O. & KHAROUFEH, J. P. 2006. Bluetooth Inquiry Time Characterization and Selection. *Mobile Computing, IEEE Transactions on,* 5**,** 1173-1187.

PORTER, D. J., KIM, D. S., MAGAÑA, M. E., POOCHAROEN, P. & ARRIAGA, C. A. G. 2011. Antenna characterization for bluetooth-based travel time data collection. *Transportation Research Board 90th Annual Meeting*

SAWANT, H., JINDONG, T., QINGYAN, Y. & QIZHI, W. Using Bluetooth and sensor networks for intelligent transportation systems. Intelligent Transportation Systems, 2004. Proceedings. The 7th International IEEE Conference on, 3-6 Oct. 2004 2004. 767-772.

SIG. 2010. *Specification of Bluetooth system* [Online]. Available: http://www.bluetooth.com/pages/smart-logos-manufacturers.aspx [Accessed December 2012.

SORIGUERA, F. & ROBUSTÉ, F. 2011. Estimation of traffic stream space mean speed from time aggregations of double loop detector data. *Transportation Research Part C: Emerging Technologies,* 19**,** 115-129.

SUN, C., RITCHIE, S. G., TSAI, K. & JAYAKRISHNAN, R. 1999. Use of vehicle signature analysis and lexicographic optimization for vehicle reidentification on freeways. *Transportation Research Part C: Emerging Technologies,* 7**,** 167-185.

TSUBOTA, T., BHASKAR, A., CHUNG, E. & BILLOT, R. 2011. Arterial traffic congestion analysis using Bluetooth duration data. *Australasian Transport Research Forum 2011.*

VAN BOXEL, D., SCHNEIDER, W. & BAKULA, C. 2011. Innovative Real-Time Methodology for Detecting Travel Time Outliers on Interstate Highways and Urban Arterials. *Transportation Research Record: Journal of the Transportation Research Board,* 2256**,** 60-67.

VAN LINT, J. W. C., HOOGENDOORN, S. P. & VAN ZUYLEN, H. J. 2005. Accurate freeway travel time prediction with state-space neural networks under missing data. *Transportation Research Part C: Emerging Technologies,* 13**,** 347-369.

VO, T., SUH, W., GUENSLER, R., GUIN, A., HUNTER, M. P. & RODGERS, M. O. 2012. Assessment of multi-antenna array performance for detecting bluetooth enabled 2 devices in a traffic stream. *Transportation Research Board 91st Annual Meeting*

WANG, Y., MALINOVSKIY, Y., WU, Y.-J. & LEE, U. K. 2011. Error Modeling and Analysis for Travel Time Data Obtained from Bluetooth MAC Address Matching. Department of Civil and Environmental Engineering University of Washington.

ZHANG, X. & RICE, J. A. 2003. Short-term travel time prediction. *Transportation Research Part C: Emerging Technologies,* 11**,** 187-210.

LIST OF TABLES

Table 1: Bluetooth classification

Class	Range (m)	Radio frequency power output (max)	Comment
Class-1	100	20 dBm	Primarily for industrial use
Class-2	10	4 dBm	Most commonly found in mobile phones, car navigation etc.
Class-3	1	0 dBm	For very short range devices such as keyboard, mouse, etc.

Table 2: Sample BMS data from Brisbane, Australia. Here, *Number* is the record number; *Device ID* is encrypted MAC-ID of the BT device; *Intersection ID* is the ID of the intersection where BMS is located; *Time-stamp* is the time when the device is first discovered; and *Duration* is the time difference between the last and first discoveries of a BT device at the respective BMS location

Number	Device ID	Intersection ID	Timestamp	Duration (seconds)
1	10	10087	2011/08/04 09:23:26	84
2	25	10087	2011/08/04 09:42:15	14
3	33	10087	2011/08/04 11:32:07	30

Table 3: Symbol/abbreviations used in the paper

Symbol/Abbreviation	**Meaning** (*see* Figure 6)
τ_A	Time when a vehicle actually arrives at a BMS zone
τ'_A	Arrival time of a vehicle from a BMS data
τ_D	Time when a vehicle actually departs from a BMS zone
τ'_D	Departure time of a vehicle from BMS data
ε_A	Temporal error of a BMS in reporting of the arrival time: Time difference between the reported and actual arrival times of a vehicle at a BMS zone
ε_D	Temporal error of a BMS in reporting of the vehicle departure time: Time difference between the actual and reported departure times of a vehicle at the BMS zone
τ_{fr}	Time when a vehicle is first reported at a BMS zone
τ_{ld}	Time when a vehicle is last discovered at a BMS zone
τ_{lr}	Time when a vehicle is last reported at a BMS zone
τ_d	Time when a vehicle actually departs from a BMS zone
d'	Reported duration of a vehicle
d	Actual duration of a vehicle

LIST OF FIGURES

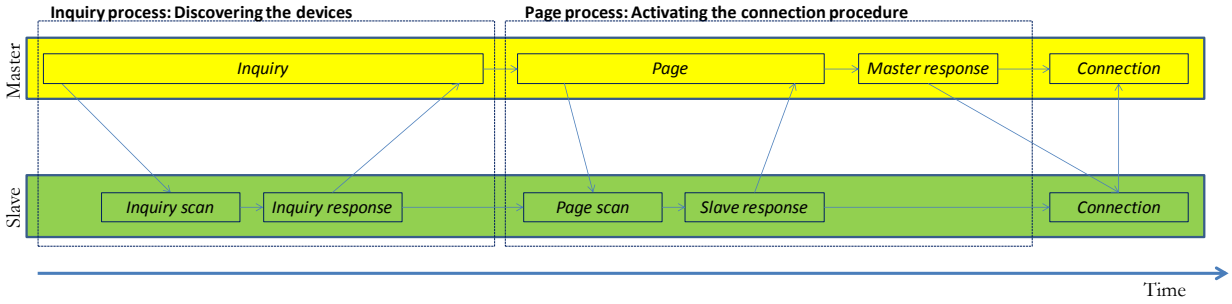

Figure 1: Simplified model for Bluetooth devices' connection procedure (Time axis is not to scale; *Inquiry* process is more time and energy consuming than *page* process)

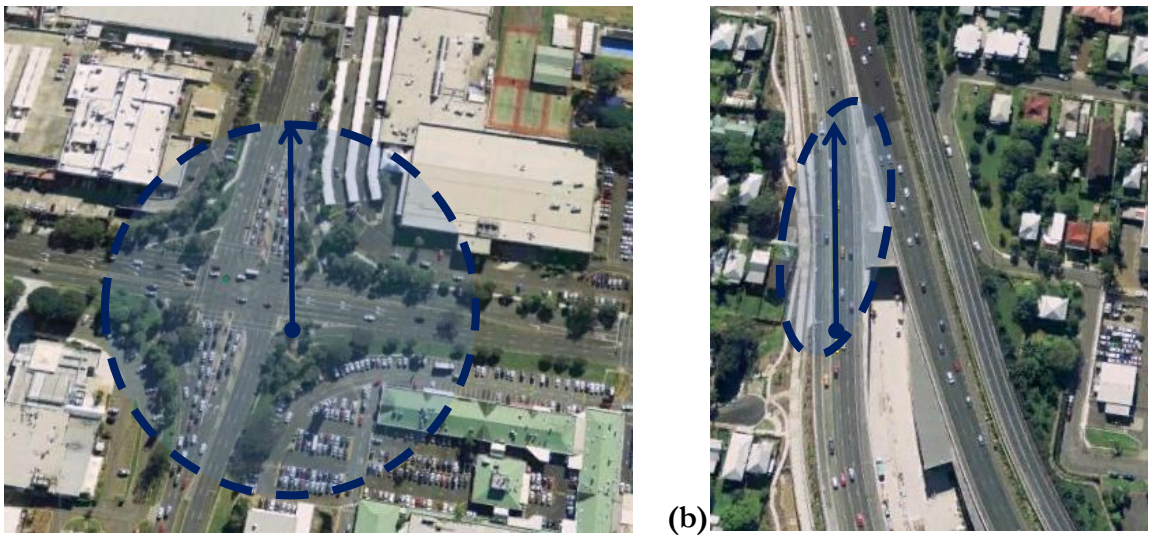

Omni-Directional antenna

Equal communication of signals over all directions.

Uni-directional antenna

Signals along one direction is maximized and other directions are suppressed.

Figure 2: Illustration of the shape and size of BMS zone (blue shaded region): a) Omni-directional antenna; and b) Uni-directional antenna

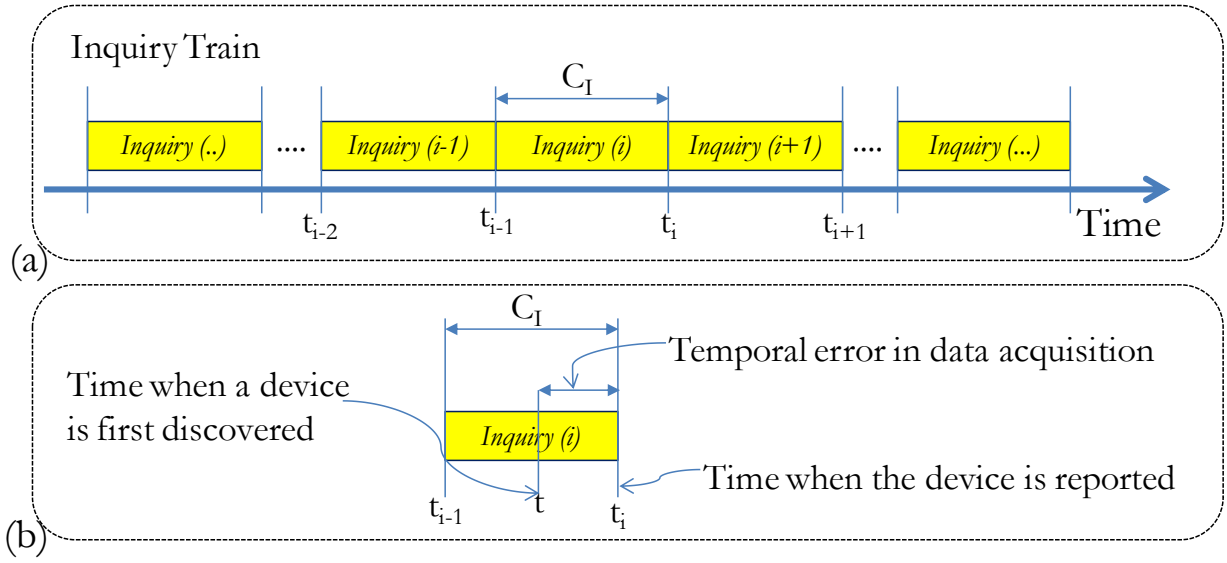

Figure 3: Illustration of an *a*) inquiry train and *b*) portion of the temporal error in data acquisition

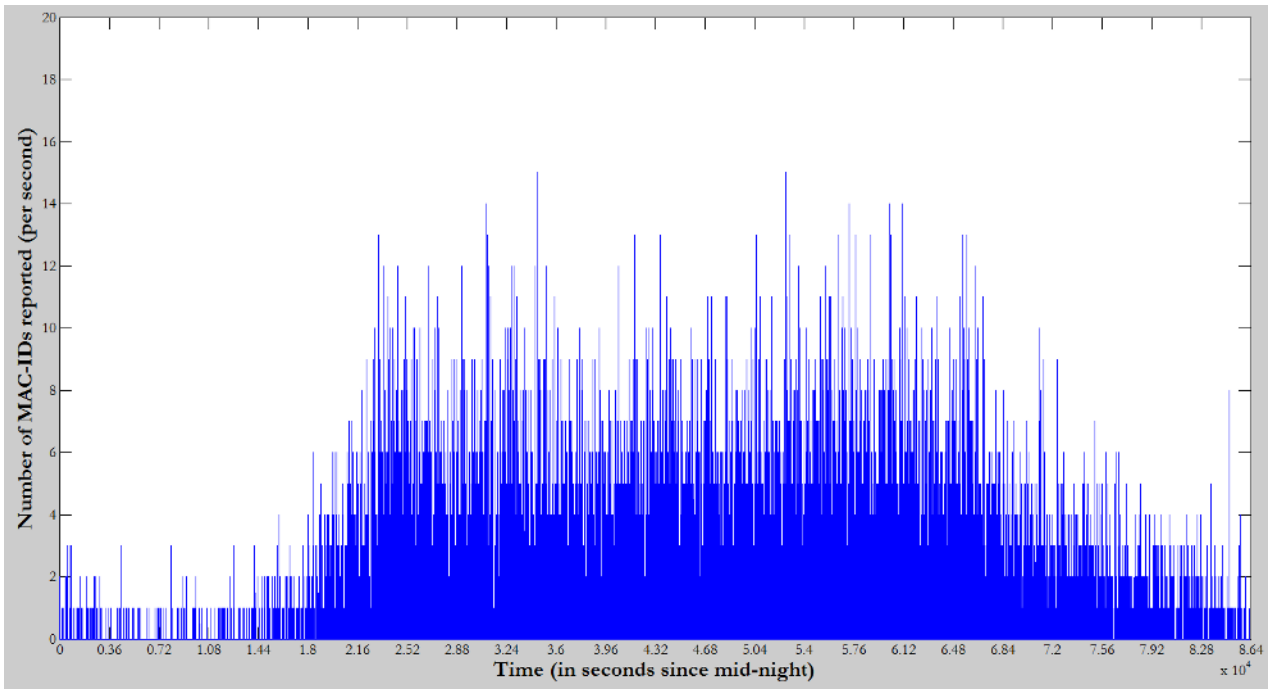

(a)

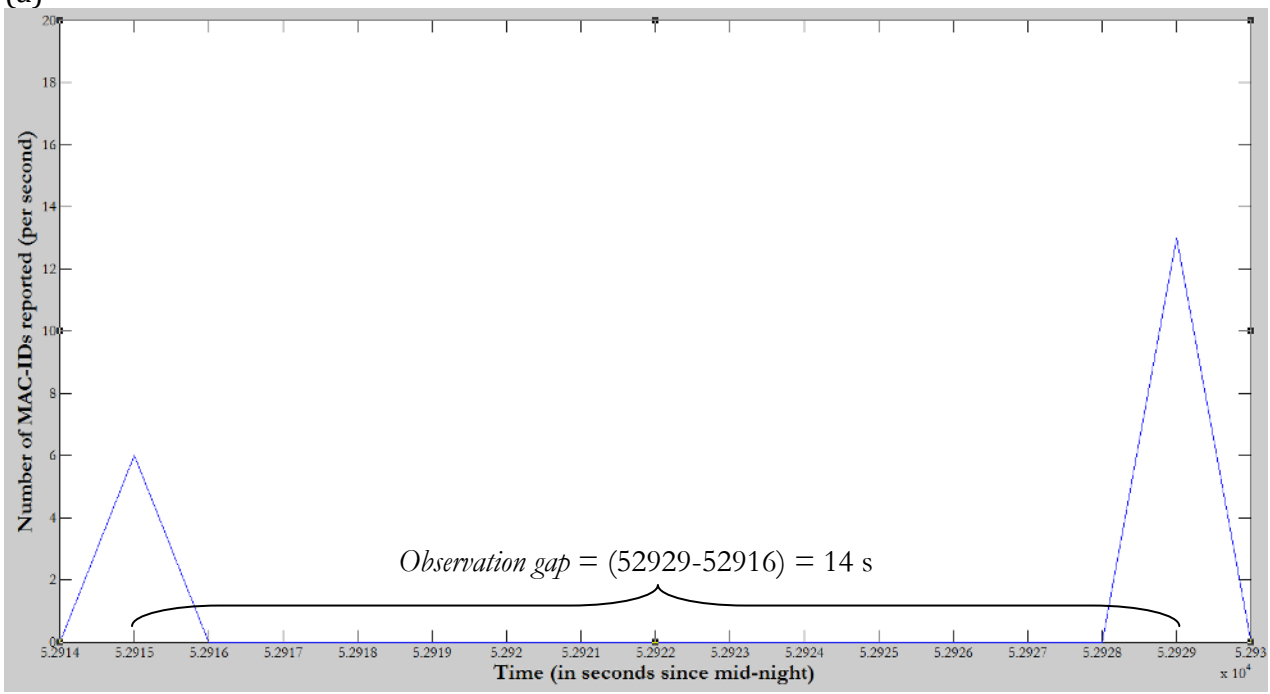

(b)

Figure 4: Time series for number of MAC records observed at a BMS location in Brisbane, Australia: a) whole day; b) zoomed in during early morning

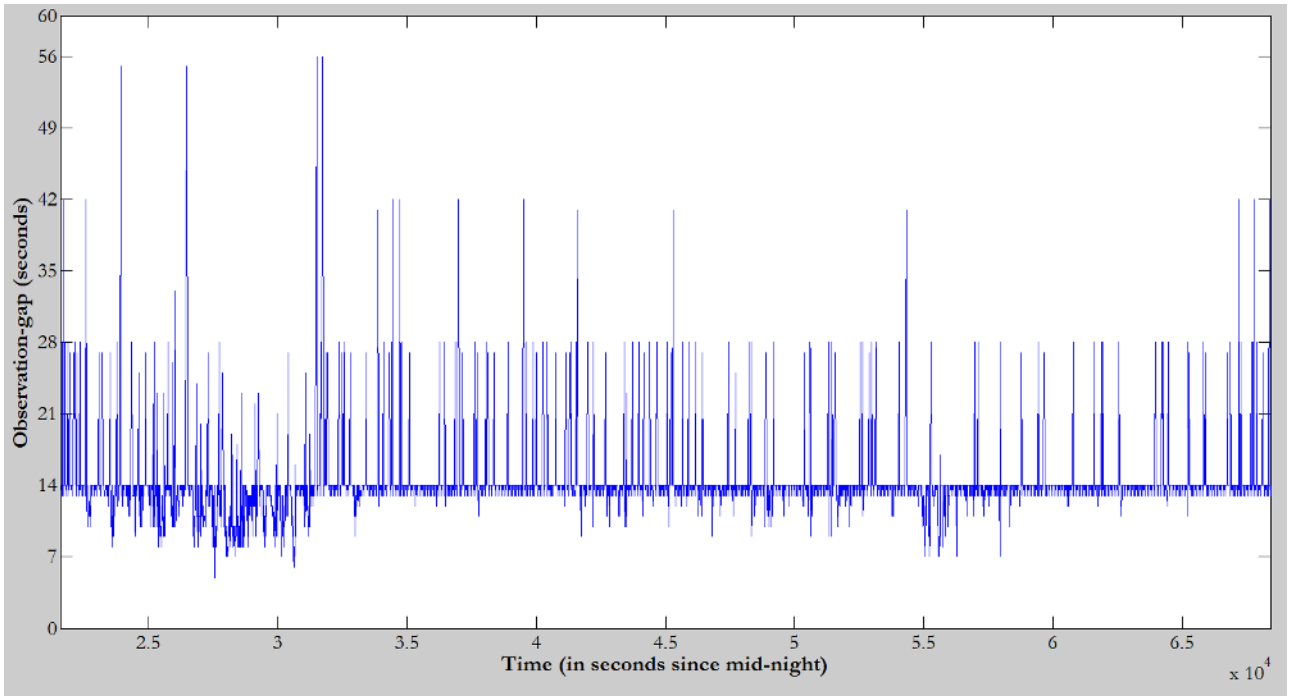

(a)

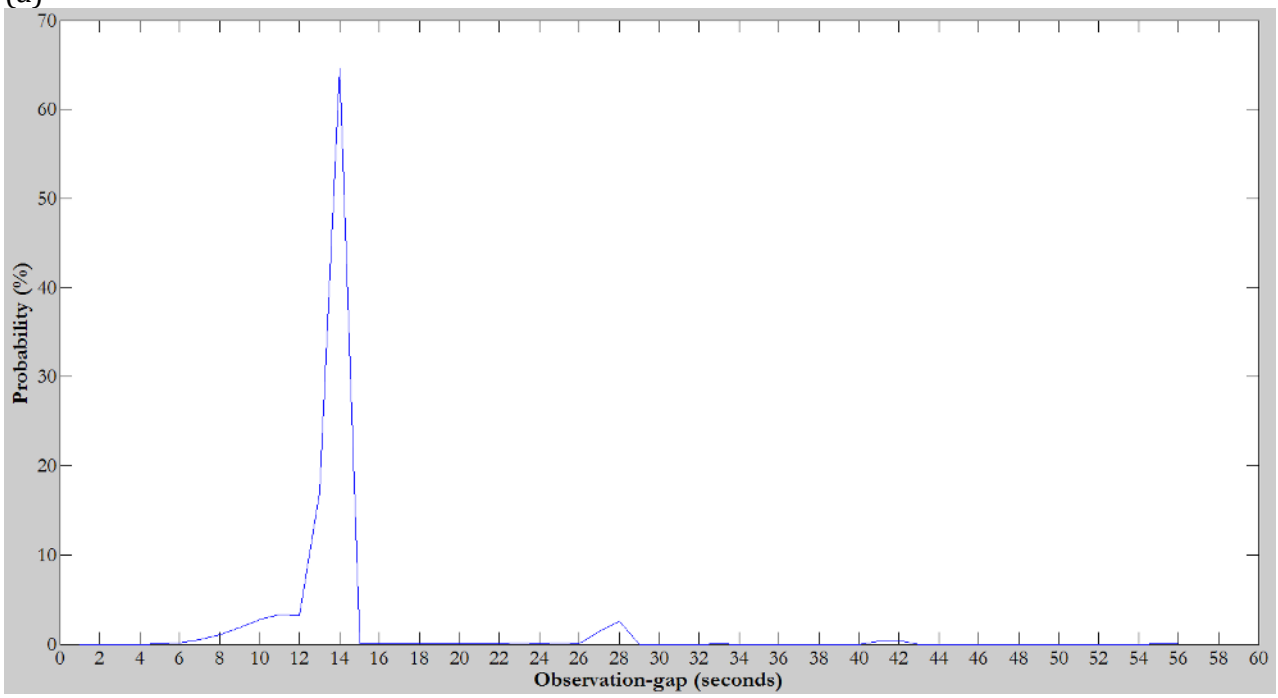

(b)

Figure 5 a) Time series of the *observation-gap* at a BMS location in Brisbane; b) Probability density of the *observation-gap* presented in *a*

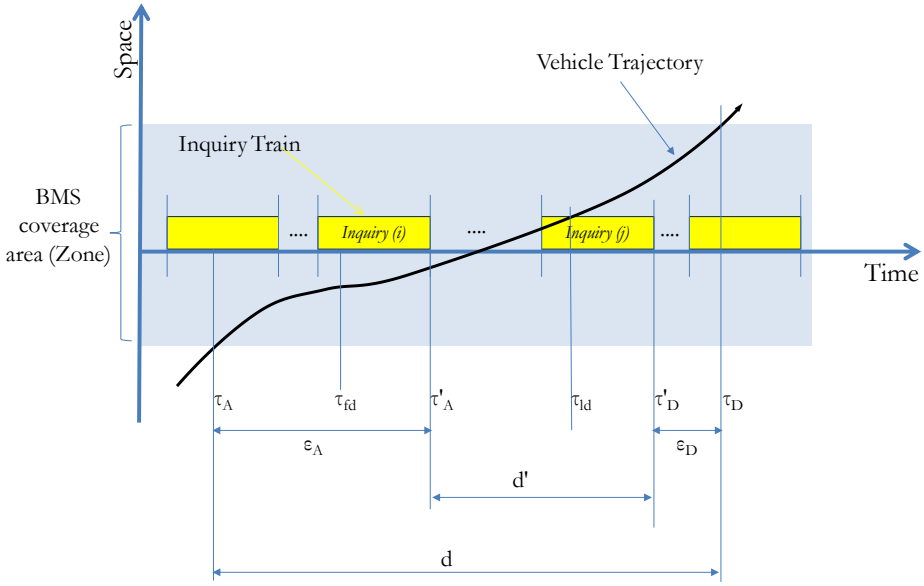

Figure 6: Time-space trajectory plot for a vehicle through a BMS zone with symbolic representation inquiry train

Figure 7: A photograph of a BMS equipped signal controlled in Brisbane with a shark fin shaped BMS antenna on the top

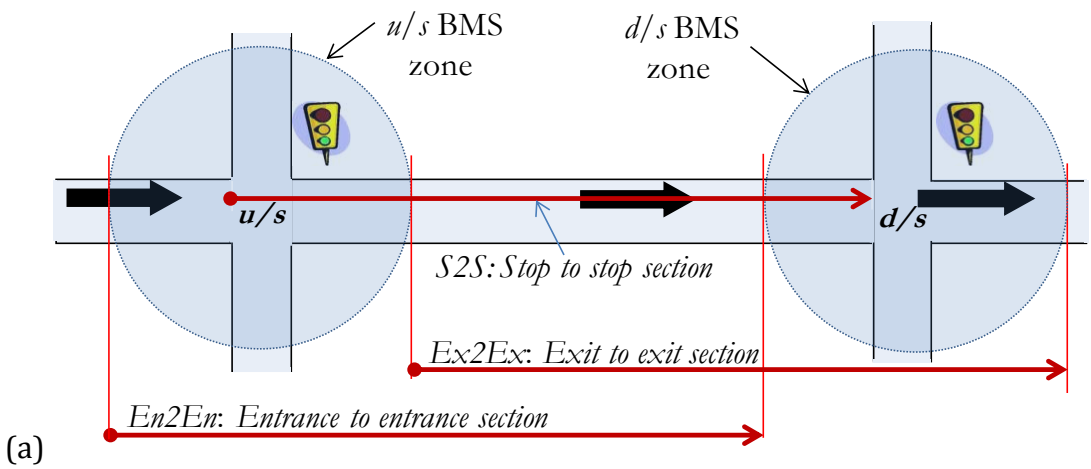

(a)

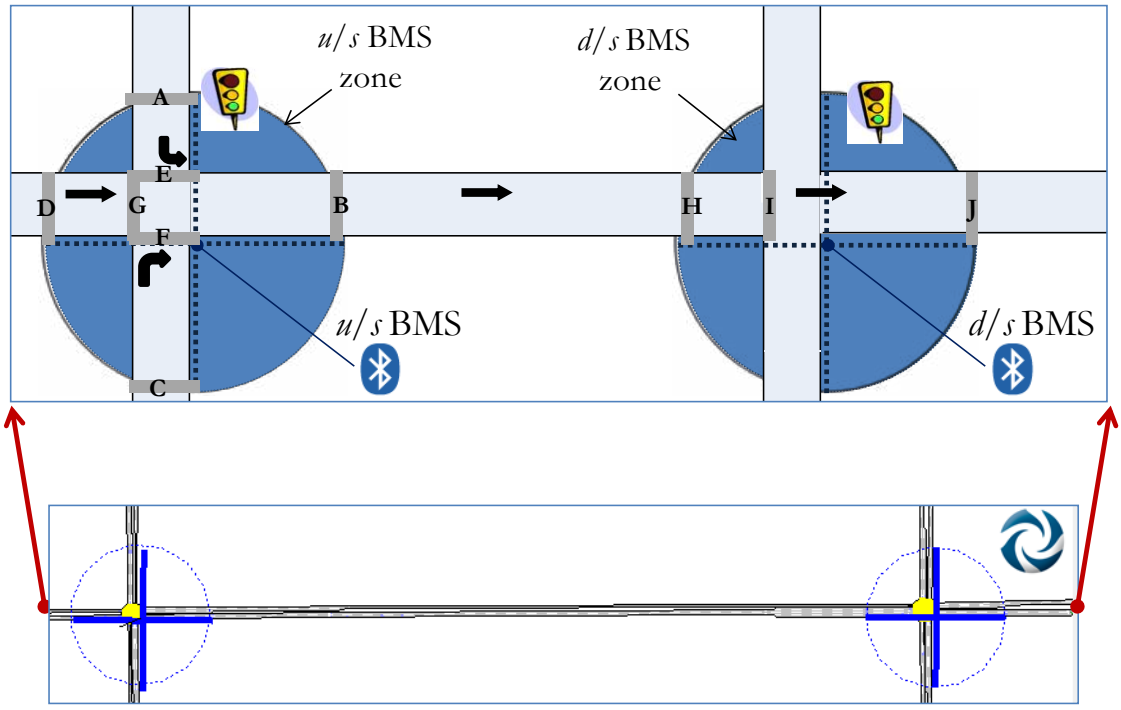

(b)

Figure 8: a) Systematic illustration of three different sections for a through traffic on an arterial network (Assuming BMS zone is circular in shape); b) Systematic illustration of the simulation model

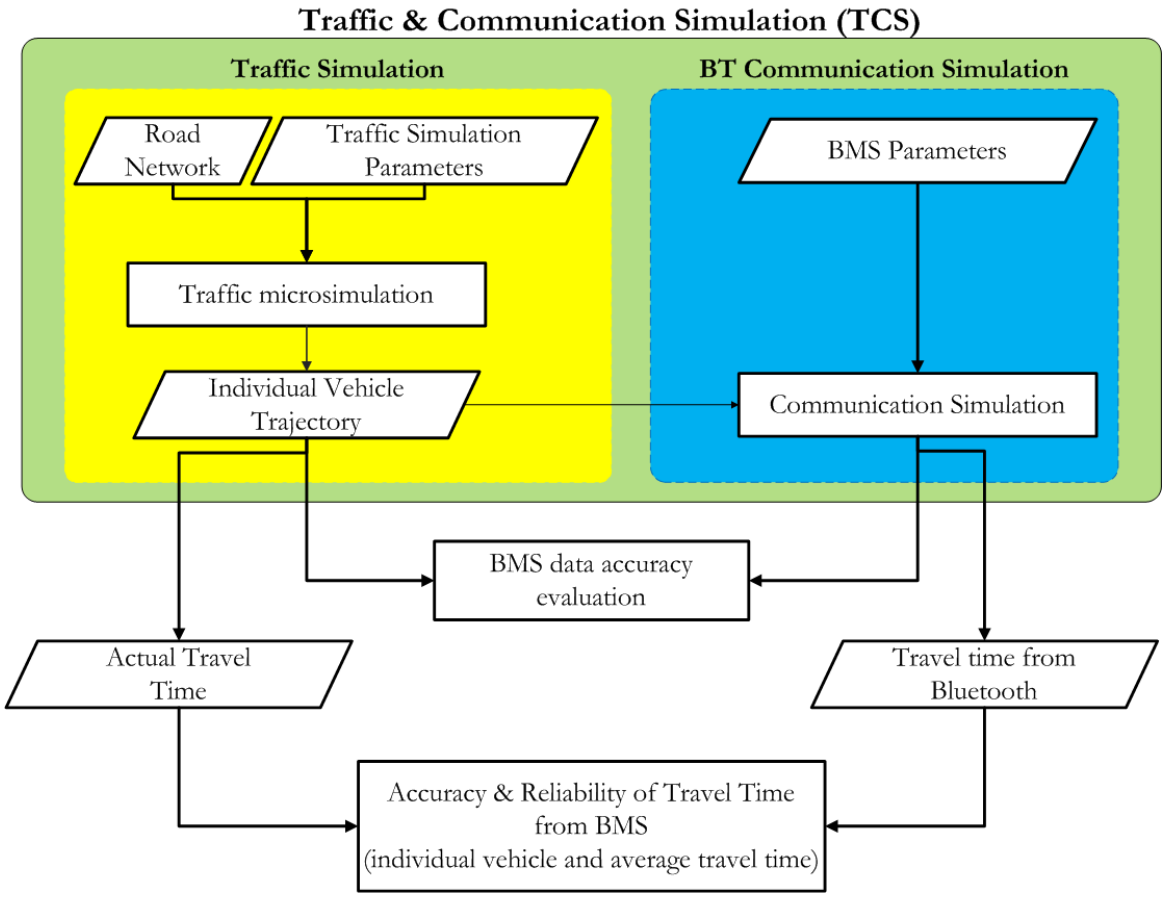

Figure 9: Traffic and communication simulation architecture; and a framework for evaluating the BMS data accuracy, and the accuracy and reliability of the travel time estimates from BMSs

(a)

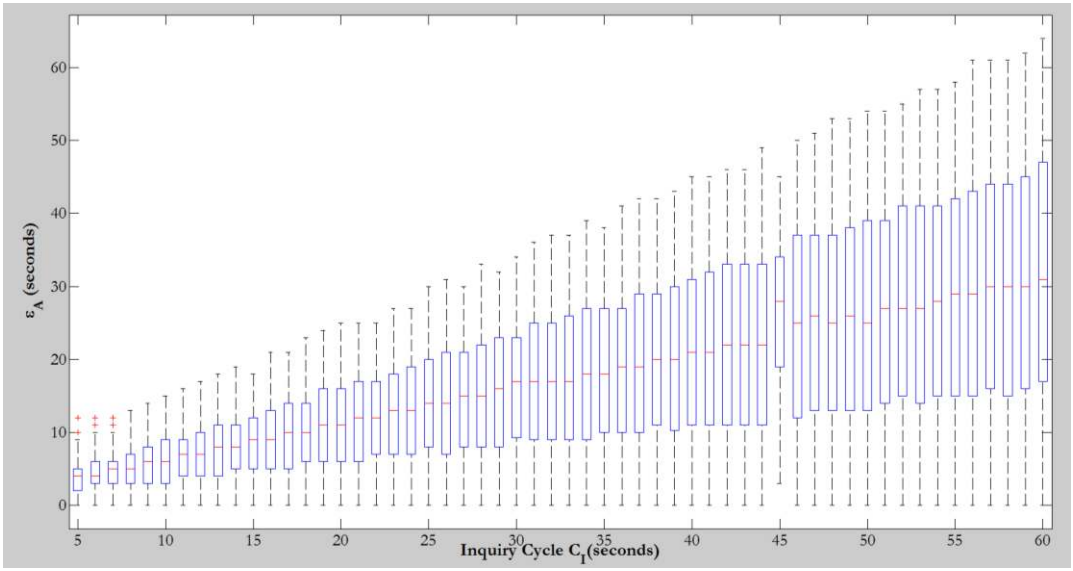

(b)

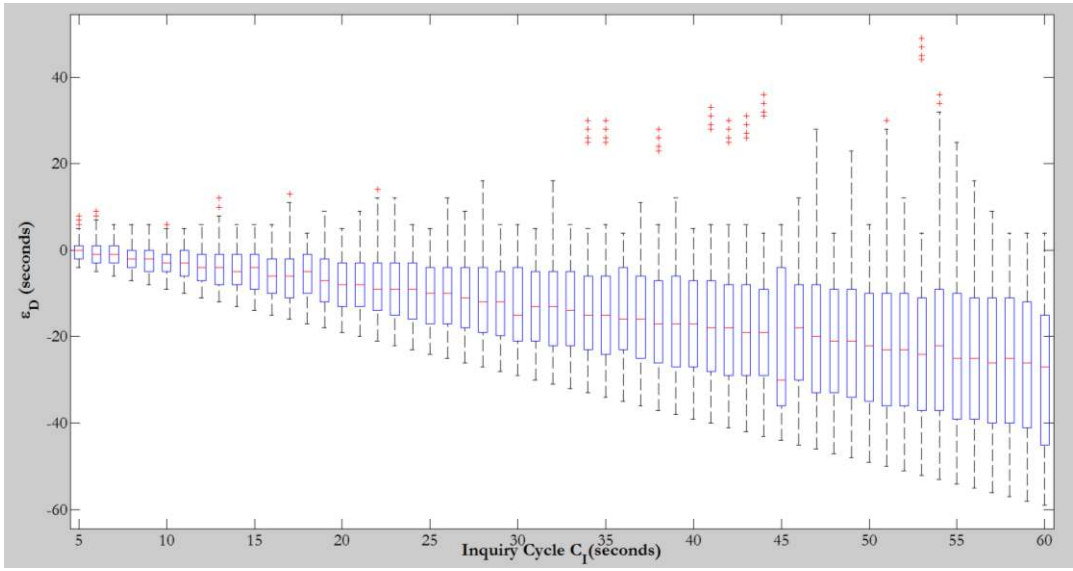

Figure 10: Box-and-whiskers plot for ε_A and ε_D versus C_I for arterial network

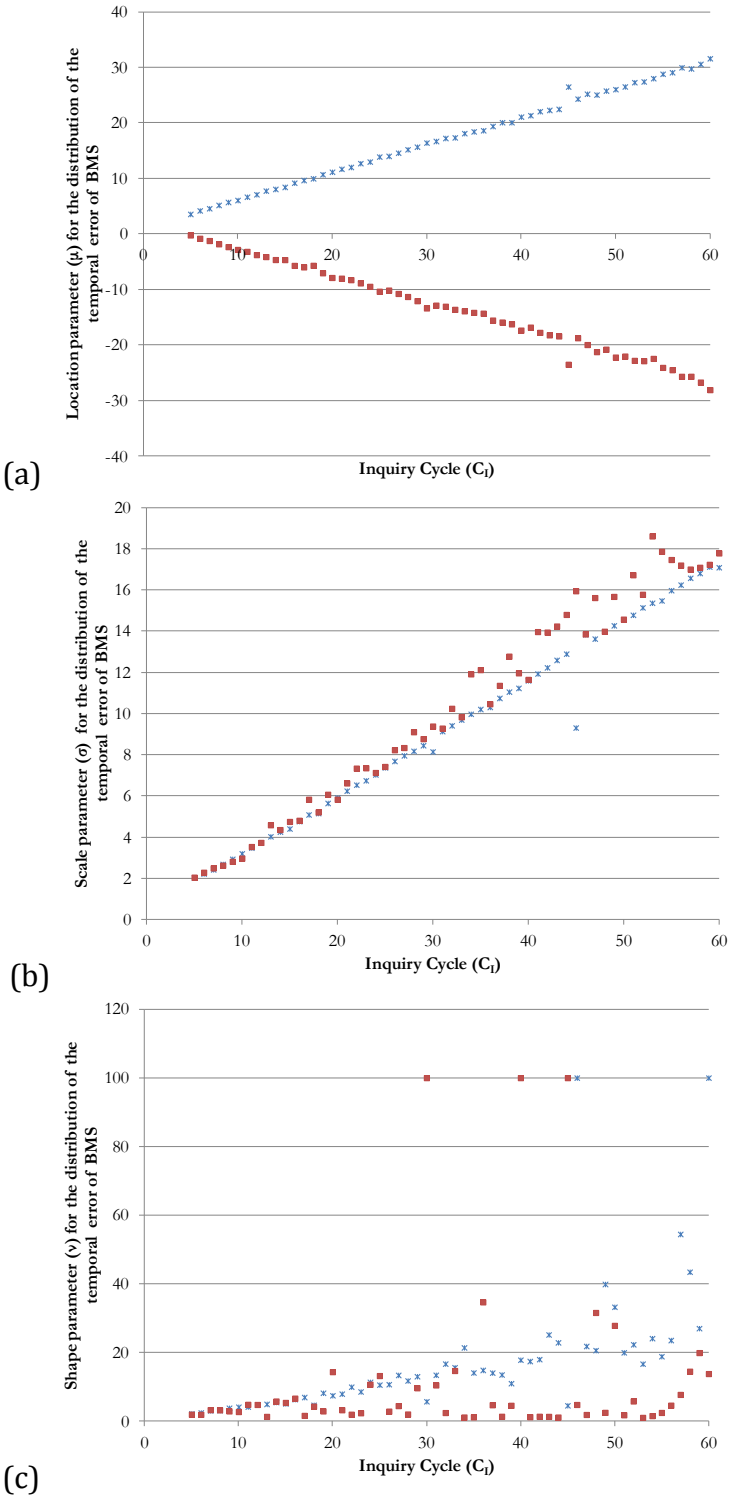

Figure 11: Temporal error distribution parameters: (a) Location parameter (μ: Mean); b) Scale parameter (σ: Standard deviation) and c) Shape parameter (v: Power index)): Star and rectangular points are for ε_A and ε_D, respectively

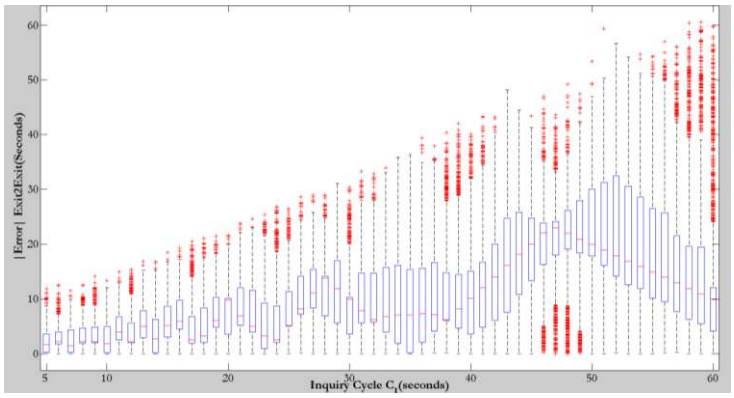

(a) Case- LL

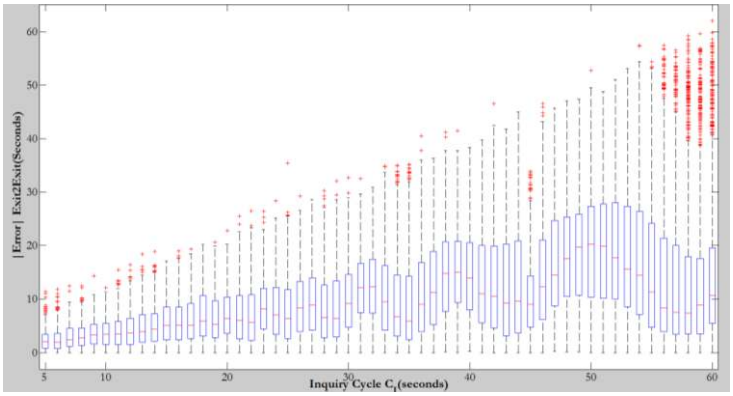

(b) Case- LM

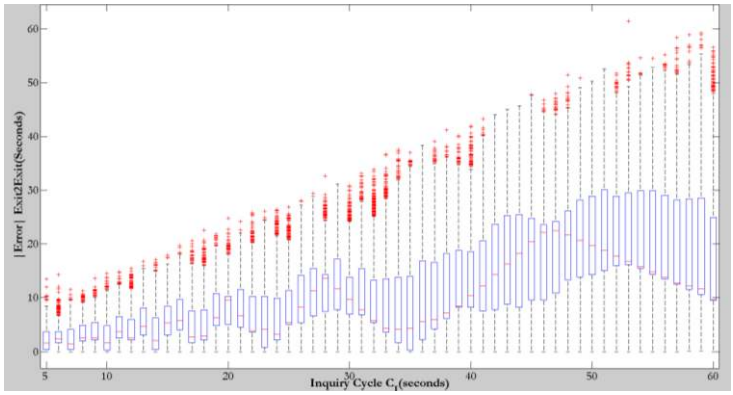

(c) Case- ML

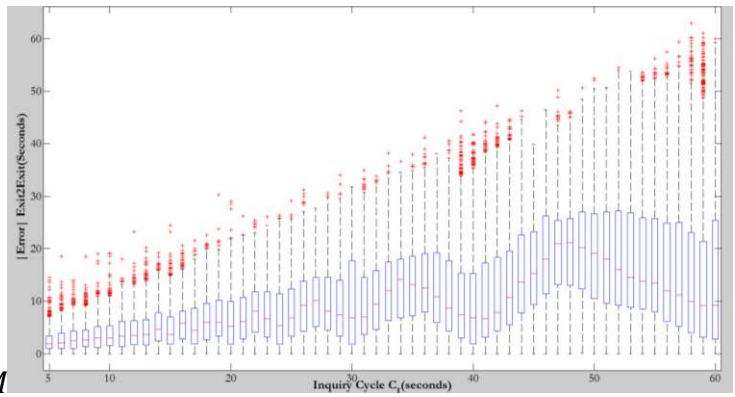

(d) Case- MM

Figure 12: Box-and-whisker plot of $|Error_{Ex2Ex}|$ versus C_I for four cases

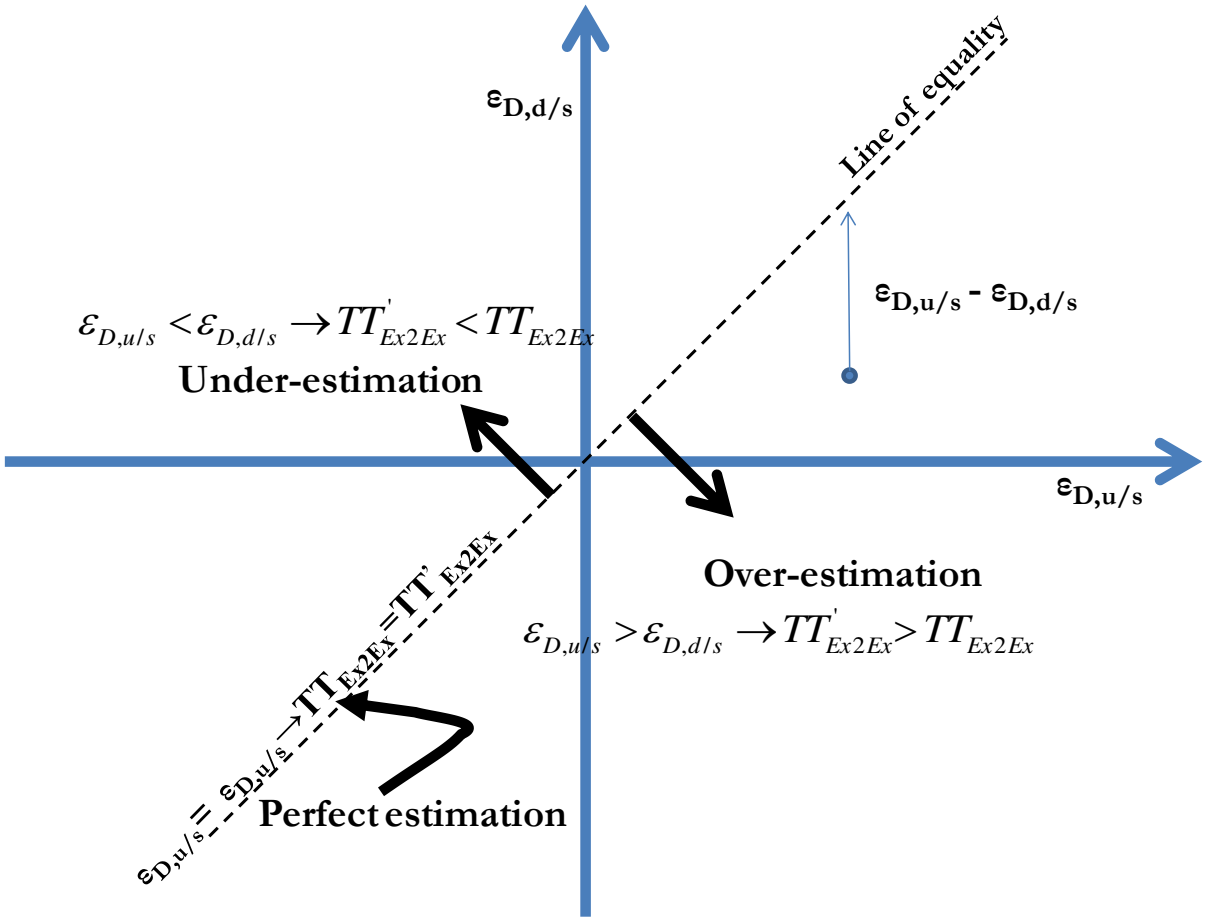

Figure 13: Representation of different regions for under-estimation, perfect and over-estimation of travel time

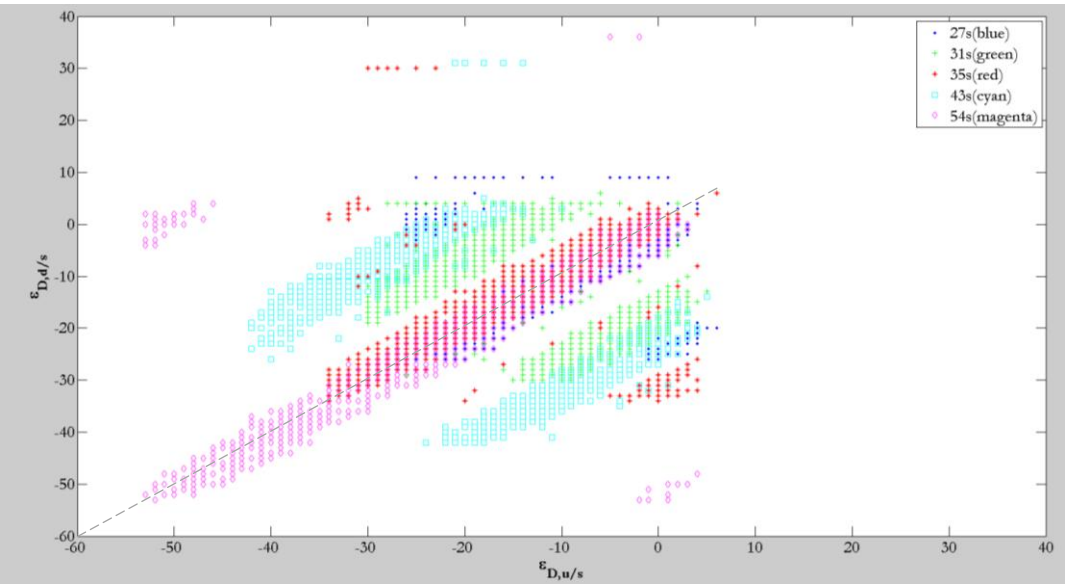

Figure 14: Sample temporal error of BMS in reporting the departure time of individual vehicles at upstream (x-axis) and downstream (y-axis) BMSs

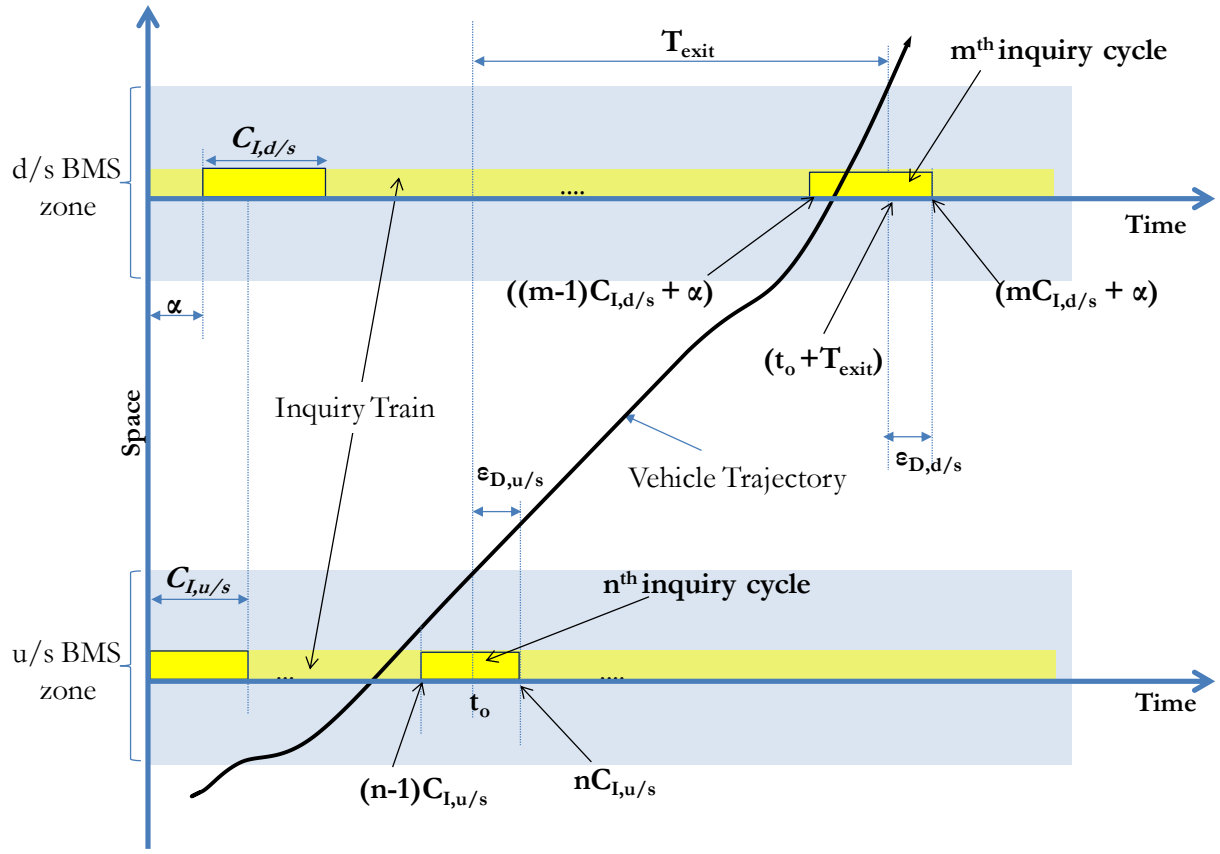

Figure 15: Illustration of a vehicle trajectory through two BMSs, where α is the offset between the two BMSs

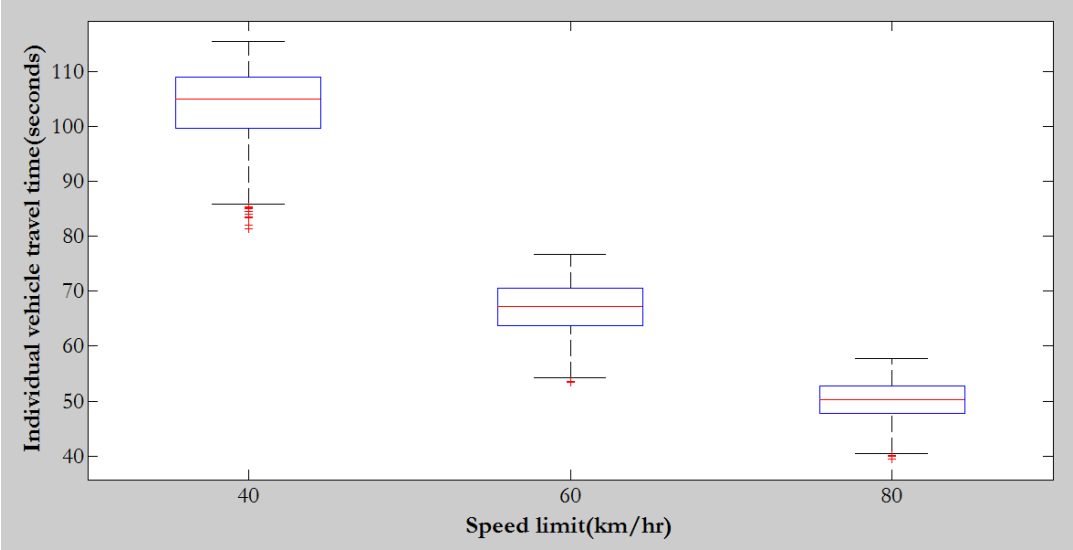

Figure 16: Box-and-whisker plot for the individual vehicle travel time versus speed limit of the free-flow network

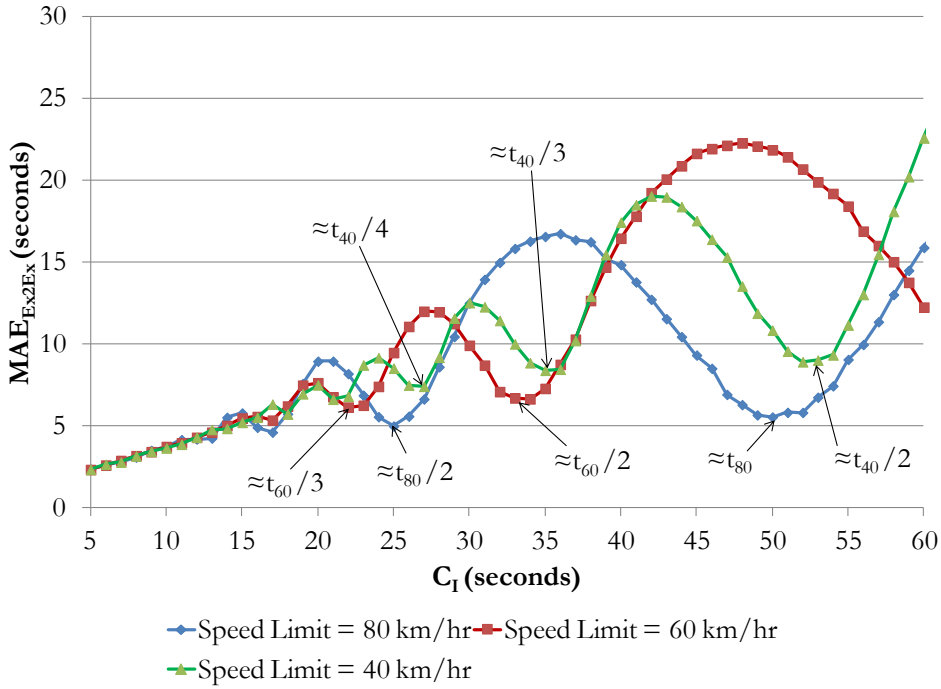

Figure 17: Mean absolute error in travel time estimation versus C_I under different speed limit under free-flow conditions

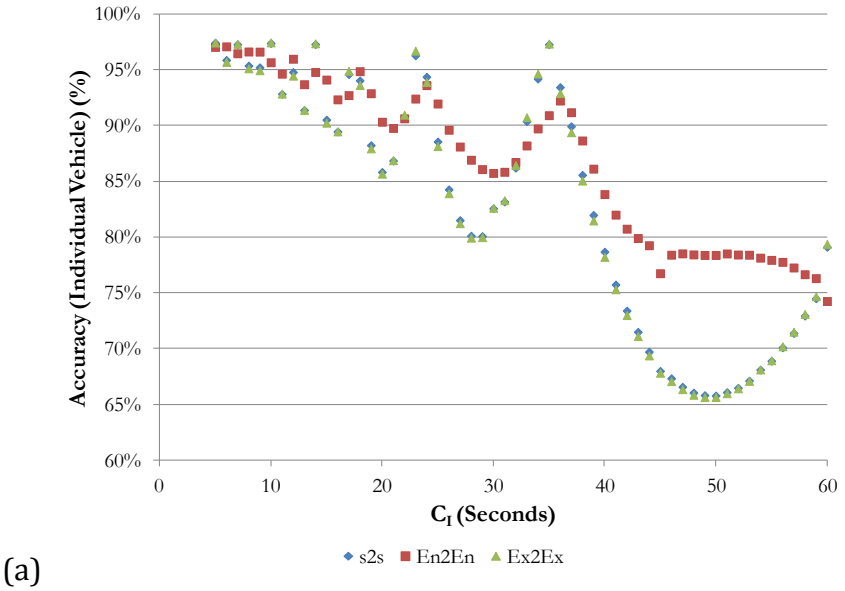

(a)

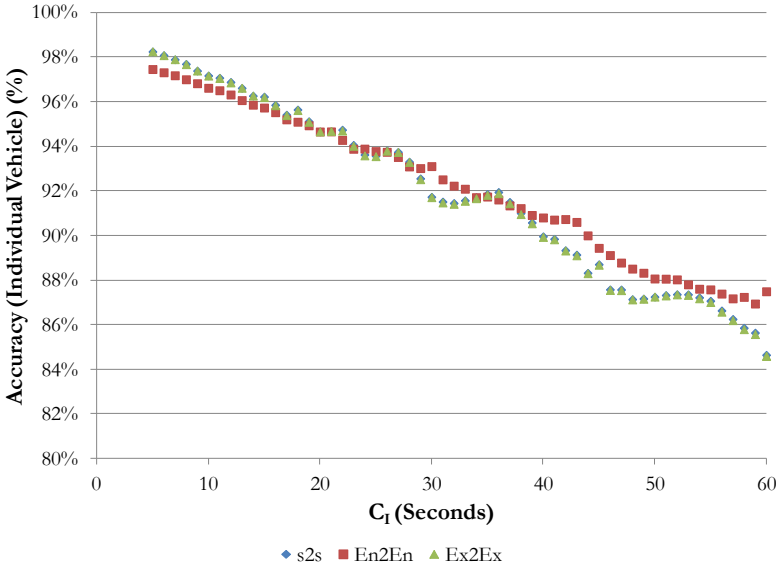

(b)

Figure 18: Accuracy for individual vehicle travel time estimation a) under-saturated conditions b) over-saturated conditions for a 1.1 km long link. (Green Triangles: Exit-to-Exit; Blue Diamonds: Stop-to-stop and Red Rectangles: Entrance-to-Entrance)

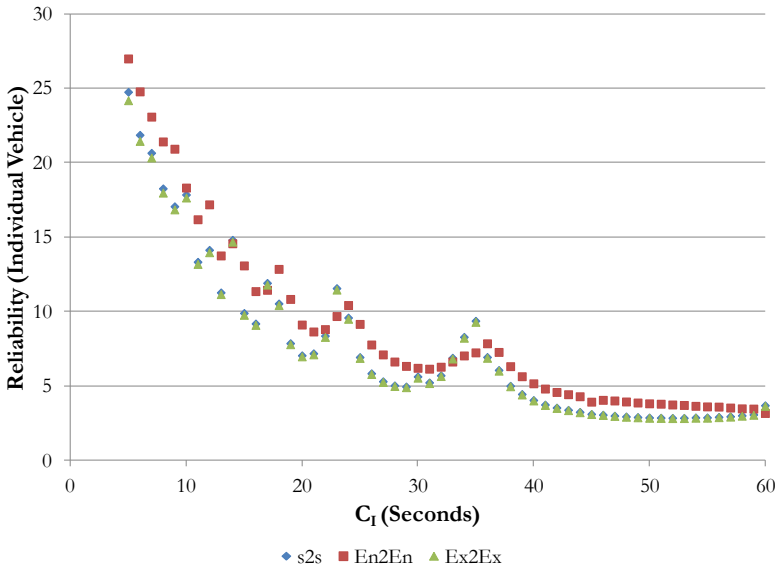

(a)

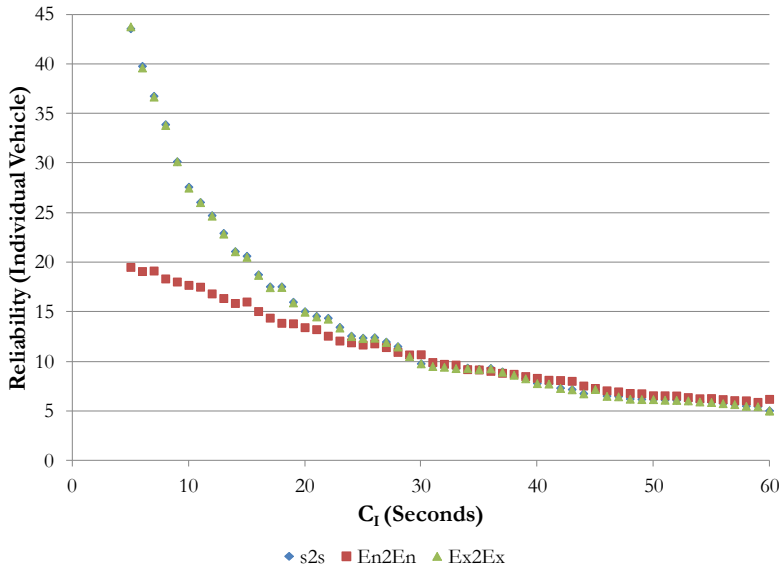

(b)

Figure 19: Reliability for individual vehicle travel time estimation a) under-saturated conditions b) over-saturated conditions for a 1.1 km long link. (Green Triangles: Exit-to-Exit; Blue Diamonds: Stop-to-stop and Red Rectangles: Entrance-to-Entrance)

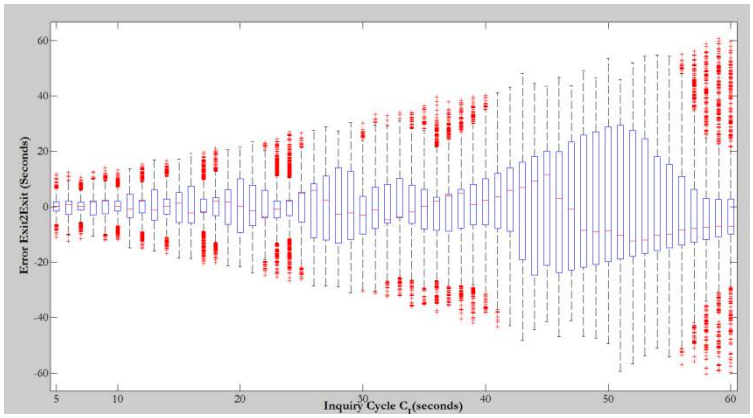

(a) Case- LL

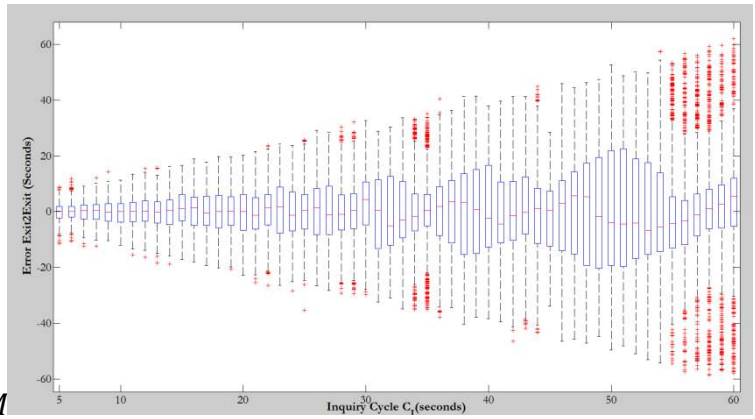

(b) Case- LM

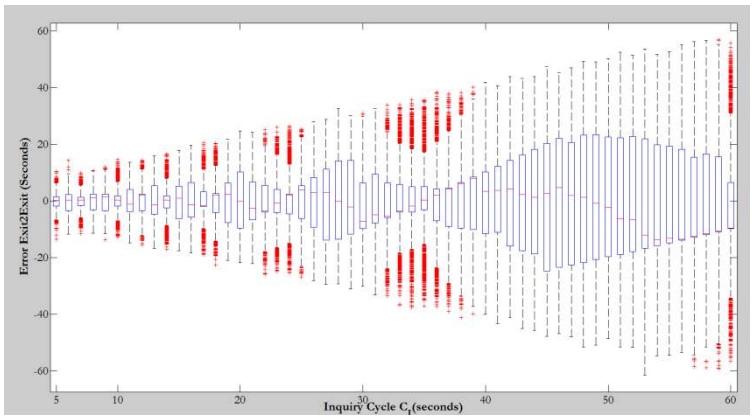

(c) Case-ML

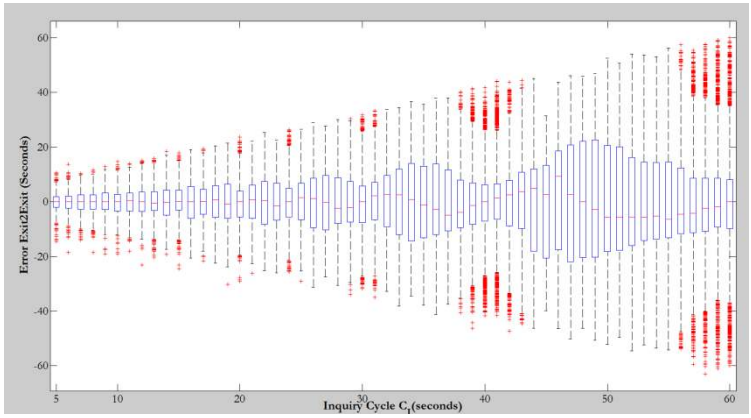

(d) Case-MM

Figure 20: Box-and-whisker plot of error for $Error_{Ex2Ex}$ versus C_I for four cases

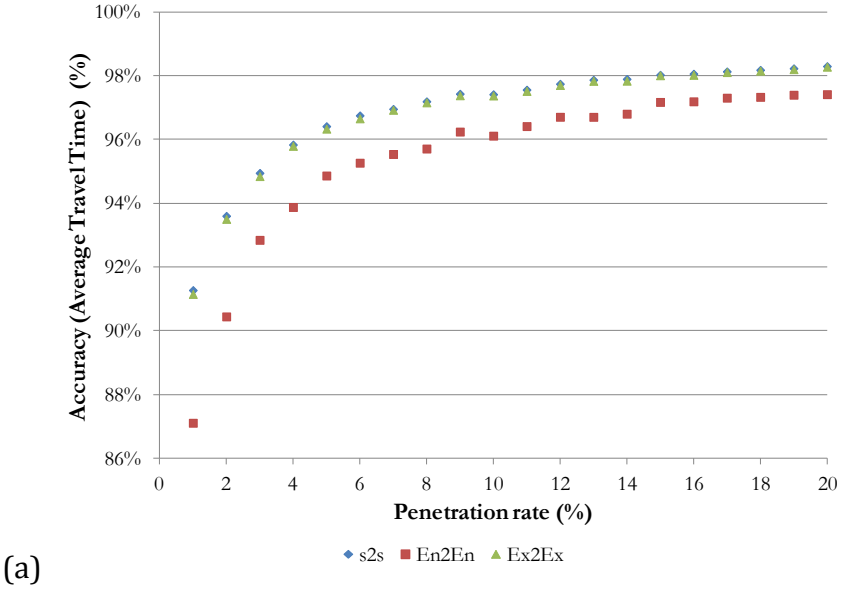

(a)

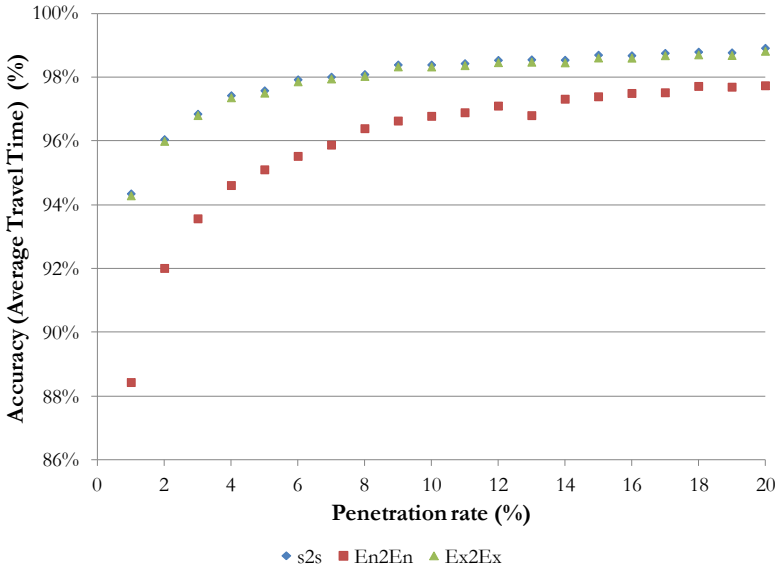

(b)

Figure 21: Accuracy (A_A) for average vehicle travel time estimation a) under-saturated conditions b) over-saturated conditions (Green Triangles: Exit-to-Exit; Blue Diamonds: Stop-to-stop and Red Rectangles: Entrance-to-Entrance)

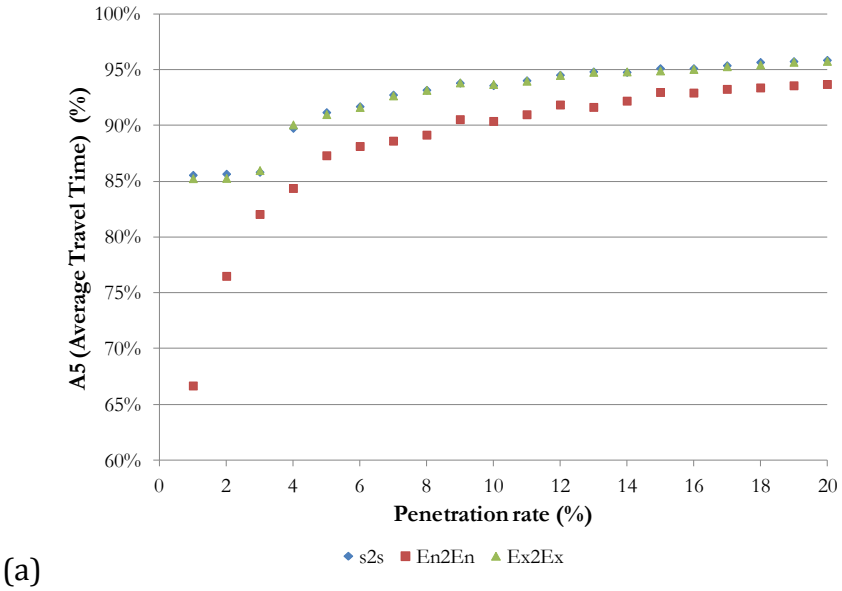

(a)

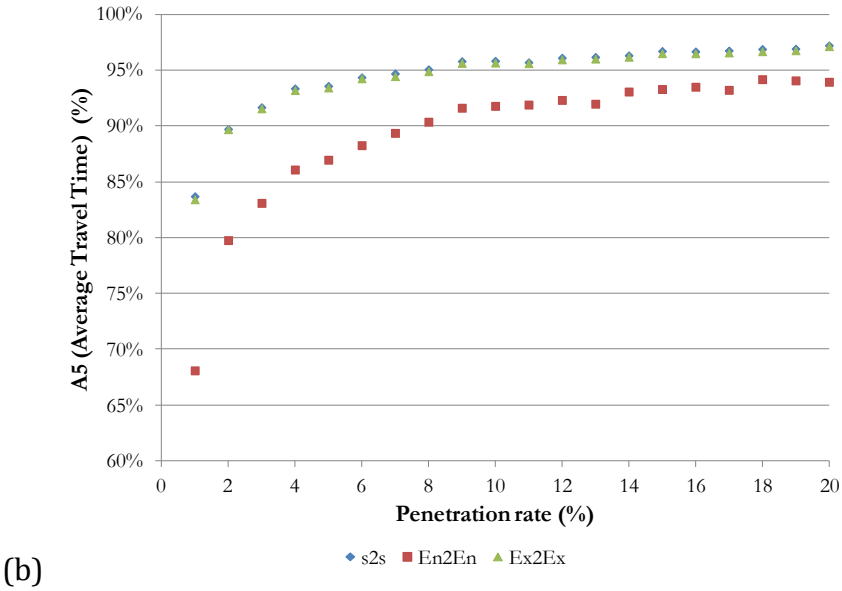

(b)

Figure 22: Accuracy (A_5) for average vehicle travel time estimation a) under-saturated conditions b) over-saturated conditions (Green Triangles: Exit-to-Exit; Blue Diamonds: Stop-to-stop and Red Rectangles: Entrance-to-Entrance)

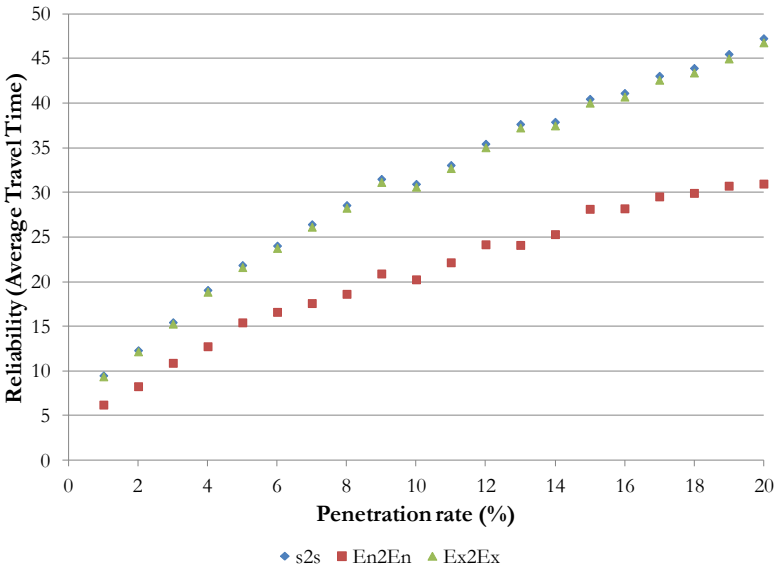

(a)

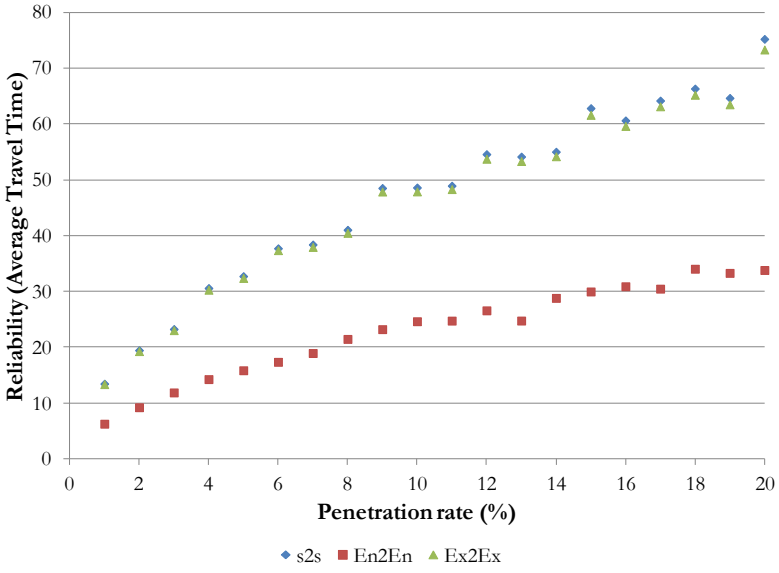

(b)

Figure 23: Reliability for average vehicle travel time estimation a) under-saturated conditions b) over-saturated conditions (Green Triangles: Exit-to-Exit; Blue Diamonds: Stop-to-stop and Red Rectangles: Entrance-to-Entrance)

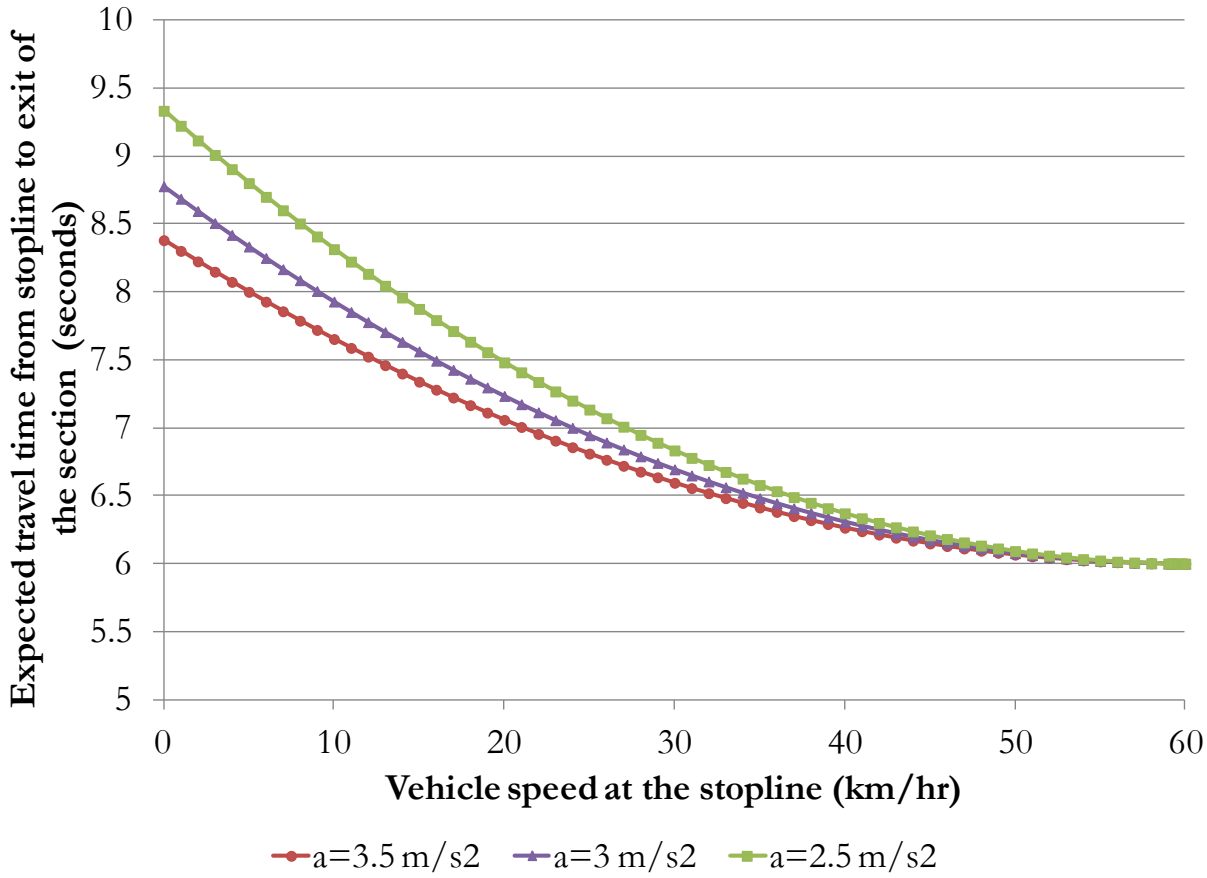

Figure 24: Expected vehicle travel time (from stop-line to exit of the section) versus initial speed of the vehicle at the stop-line

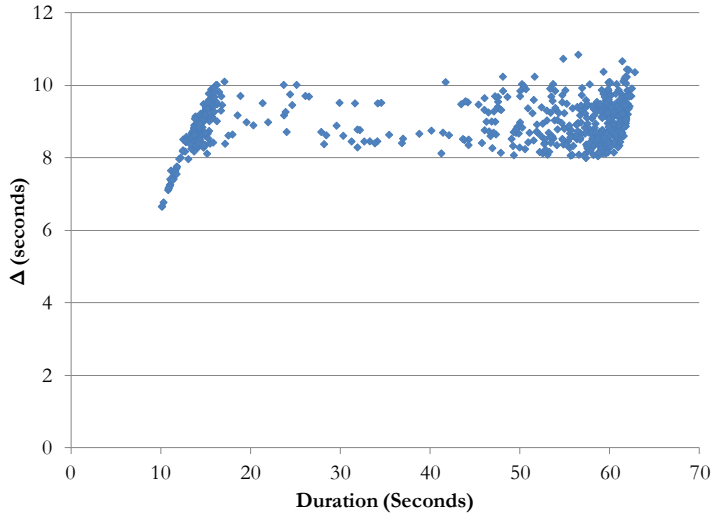

(a)

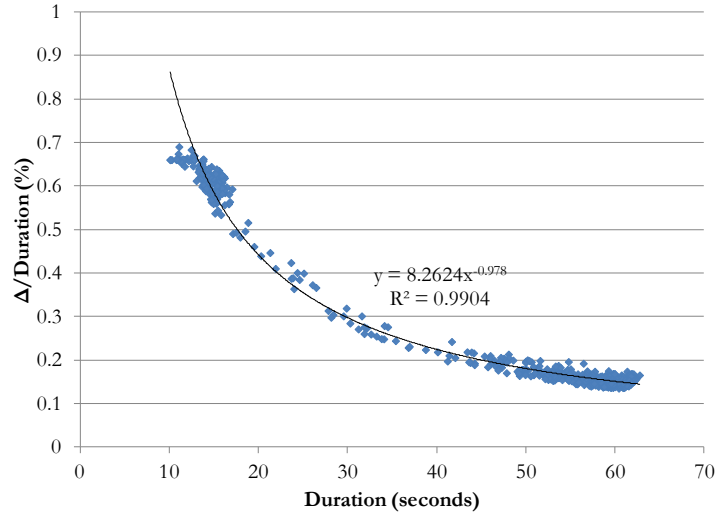

(b)

Figure 25: Relationship between the actual duration and Δ for individual vehicles on signalised arterial network

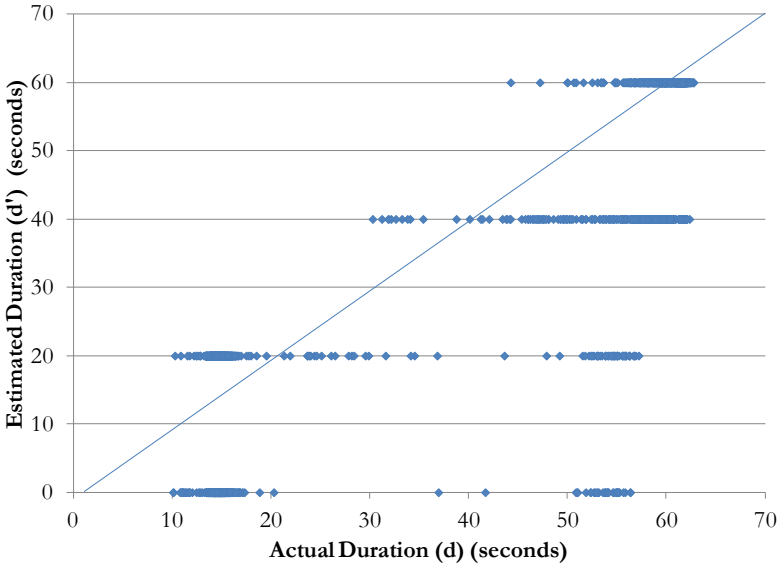

Figure 26: Relationship between estimated and actual duration

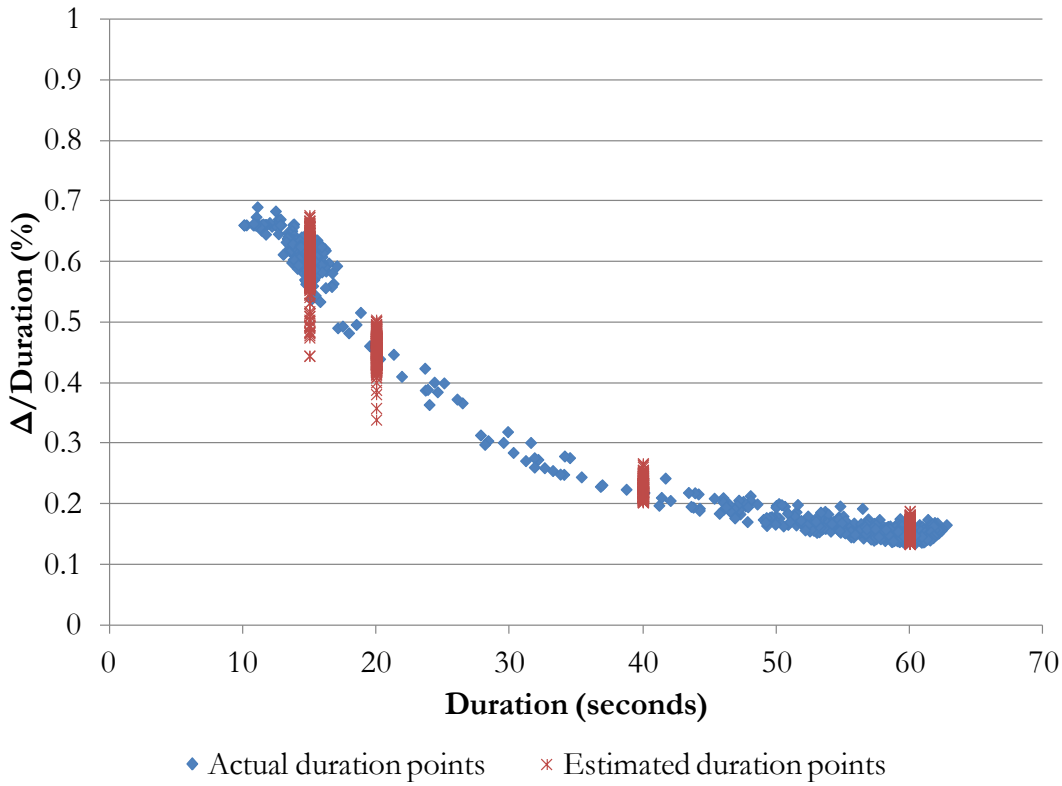

Figure 27: Relationship between the estimated duration (Red points), actual duration (Blue points) and Δ for individual vehicles on signalised arterial network.

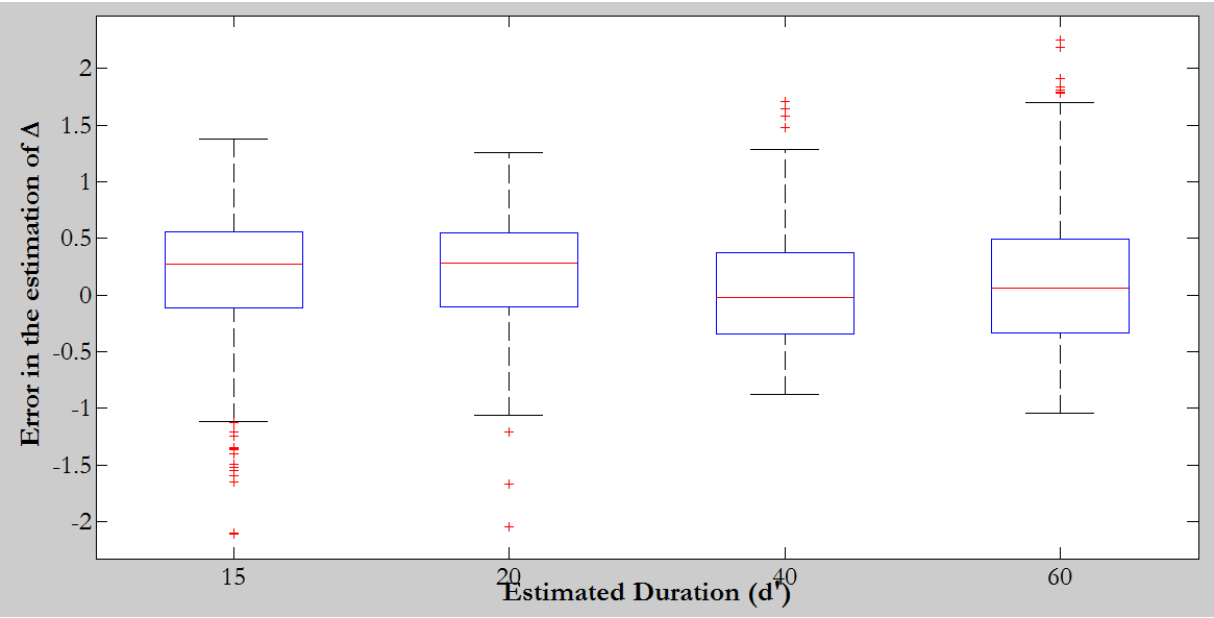

Figure 28: Box plot for error in estimation of Δ when duration data is from BMS data.

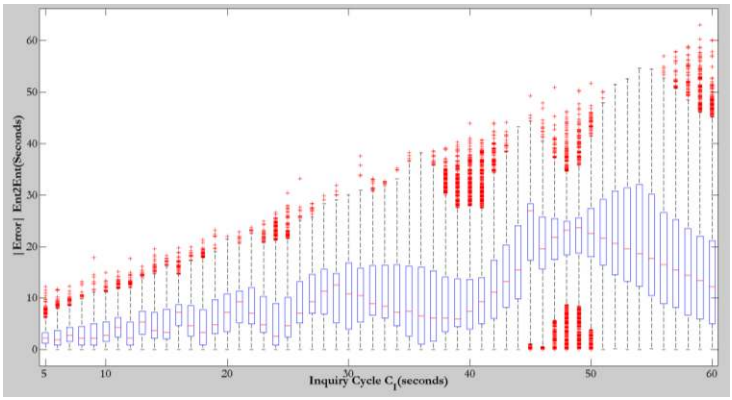

(a) Case- LL

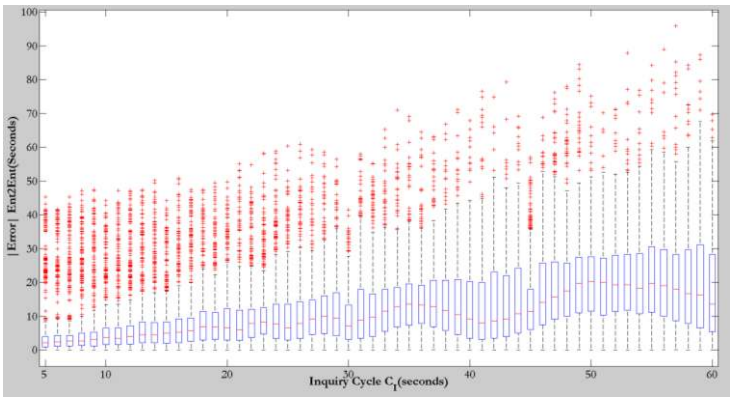

(b) Case- LM

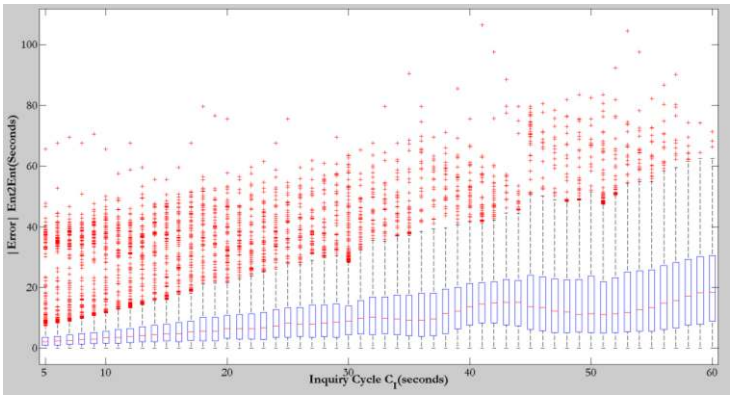

(c) Case- ML

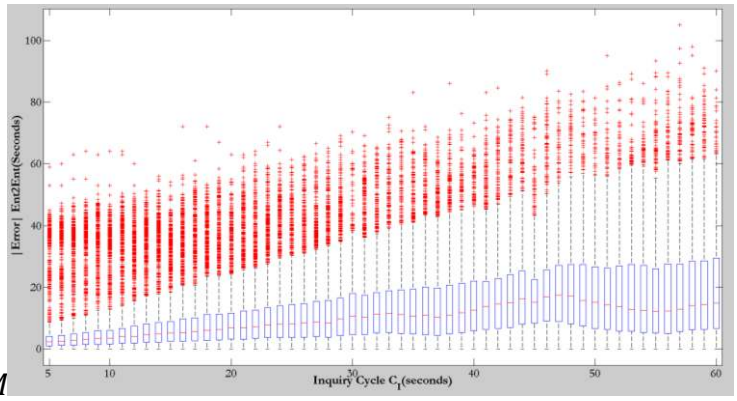

(d) Case- MM

Figure 29: Box-and-whisker plot for $|Error_{En2En}|$ versus C_I for four cases

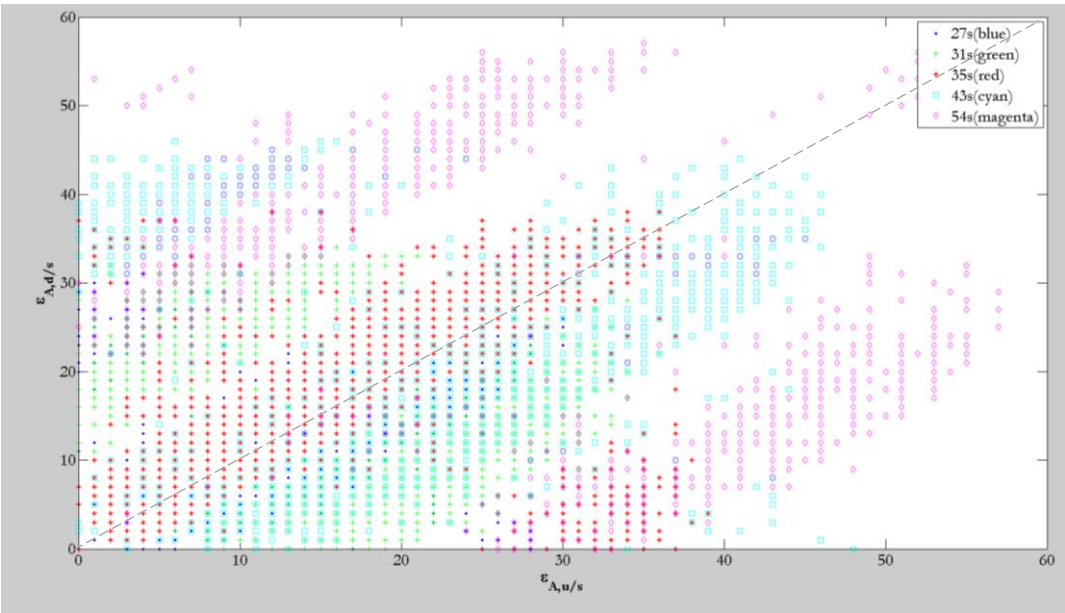

Figure 30: Sample temporal error of BMS in reporting the arrival time of individual vehicles at upstream (x-axis) and downstream (y-axis) BMSs

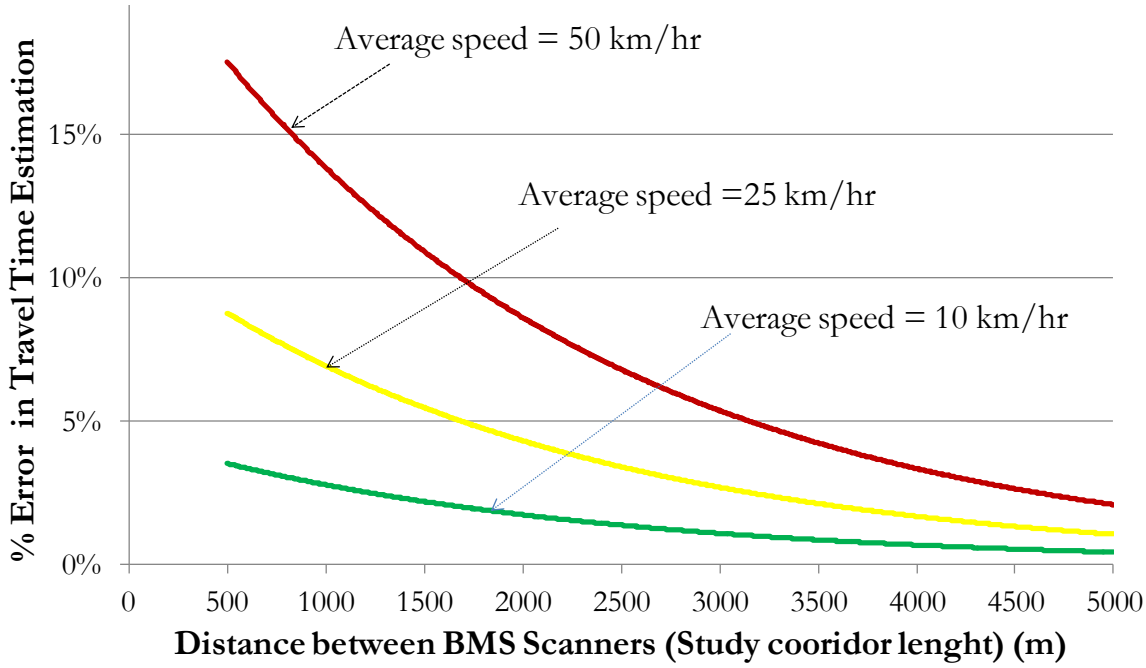

Figure 31: Illustration of the percentage error in individual vehicle travel time estimation from BMS data as function of the distance between BMS scanners and average travel speed